

Rejection Sampling with Vertical Weighted Strips

Andrew M. Raim*, James A. Livsey, and Kyle M. Irimata

Center for Statistical Research and Methodology, U.S. Census Bureau

Abstract

A number of distributions that arise in statistical applications can be expressed in the form of a weighted density: the product of a base density and a nonnegative weight function. Generating variates from such a distribution may be nontrivial and can involve an intractable normalizing constant. Rejection sampling may be used to generate exact draws, but requires formulation of a suitable proposal distribution. To be practically useful, the proposal must both be convenient to sample from and not reject candidate draws too frequently. A well-known approach to design a proposal involves decomposing the target density into a finite mixture, whose components may correspond to a partition of the support. This work considers such a construction that focuses on majorization of the weight function. This approach may be applicable when assumptions for adaptive rejection sampling and related algorithms are not met. An upper bound for the rejection probability based on this construction can be expressed to evaluate the efficiency of the proposal before sampling. A method to partition the support is considered where regions are bifurcated based on their contribution to the bound. Examples based on the von Mises Fisher distribution and Gaussian Process regression are provided to illustrate the method.

Keywords: Majorization; Finite Mixture; Partition; von Mises Fisher; Gaussian Process

1 Introduction

Consider a weighted distribution (Patil and Rao, 1978) with density

$$f(x) = f_0(x)/\psi, \quad f_0(x) = w(x)g(x), \quad \psi = \int_{\Omega} f_0(x)d\nu(x), \quad (1)$$

whose support is Ω and ν is an appropriate dominating measure. The base distribution $g(x)$ is assumed to be a normalized density. The weight function $w(x) \geq 0$ reweights density $g(x)$ on support Ω in a systematic way. The normalizing constant ψ may be intractable or impractical to compute. Distributions of the form (1) often arise as targets for which a random sample is desired. For example, in Bayesian analysis, such an f frequently involves a posterior distribution of interest, or one of its conditionals, with g arising from a prior distribution on unknown parameters θ and w from a likelihood which depends on θ . The method of rejection sampling continues to be relevant when an exact draw is desired from the target, rather than a Markov chain whose invariant distribution is the target, and no other method to directly generate draws is apparent. This work revisits the method of vertical strips to construct proposal distributions for rejection sampling with

Disclaimer: This article is released to inform interested parties of ongoing research and to encourage discussion of work in progress. Any views expressed are those of the authors and not those of the U.S. Census Bureau.

*For correspondence:

Andrew M. Raim (andrew.raim@census.gov)
Center for Statistical Research and Methodology
U.S. Census Bureau
Washington, DC, 20233, U.S.A.

weighted targets of the form (1). The resulting method provides additional flexibility which may be useful in obtaining useful samplers with little effort or very efficient samplers—in terms of computational burden and probability of rejection—with additional insight into the components.

Rejection sampling (von Neumann, 1951) offers a method of sampling from distributions that may be intractable or difficult to work with by utilizing an envelope function which bounds the unnormalized target density from above. This approach samples from the area beneath the envelope and rejects draws which fall above the target density and produces accepted draws which are independent and identically distributed from the target density (Robert and Casella, 2004; Martino et al., 2018a). Many types of proposal densities have been introduced to form the envelope used for generating draws. One such method utilizes a stepwise proposal (Ahrens, 1993, 1995; Pang et al., 2002) which can be regarded as a construction by vertical strips (Martino et al., 2018b, Section 3.6.1). Devroye (1986, Chapter VIII) discusses what is essentially the vertical strip method although non-adaptive and for log-concave densities. Another class of methods which is based on construction of a proposal by horizontal strips is referred to as the ziggurat method (Marsaglia and Tsang, 2000). This approach uses a set of rectangles to form the envelope, with the accuracy of the approximations improving as the number of rectangles increases (Martino et al., 2018b, Section 3.6.1). Other methods for creating proposal distributions are considered in the literature such as exponential proposals where the idea is to use exponential functions as the proposal density, making the acceptance-rejection step more tractable.

In practice, selection of an appropriate envelope for rejection sampling faces two main challenges: the envelope must be guaranteed to be an upper bound for the target density, and selection of too large an envelope will yield an inefficient sampler with many of the proposed draws rejected. Adaptive rejection sampling methods attempt to address the challenges for log-concave targets by automatically adapting to the target distribution using rejected draws, thus yielding an envelope that provides an increasingly tight bound to the target (Gilks and Wild, 1992). The Adaptive Rejection Metropolis Sampling (ARMS) drops the log-concave restriction and uses a Metropolis step (Gilks et al., 1995). However, it produces a chain of non-independent draws, and the proposal is not guaranteed to converge to the target with adaptations. The adaptive independent sticky MCMC, introduced by Martino et al. (2018a), extended this ARMS method using non-parametric adaptive proposal densities to reduce the computational burden and improve convergence. The Independent Doubly Adaptive Rejection Metropolis Sampling (IA2RMS) algorithm addresses the ARMS convergence issue and reduces dependence (Martino et al., 2015). Evans and Swartz (1998) proposed a sampler which relaxes the log-concavity requirement, and requires that a given transformation of the target density is concave. Another variation of this idea is the convex-concave ARS introduced by Görür and Teh (2011) which separates the target distribution into concave and convex functions. In addition to the above, many other adaptive rejection samplers have been introduced in the literature, Martino et al. (2018b) provide a summary of some of the most common methods.

One of the main challenges in adaptive rejection sampling lies in the construction of the sequence of proposal densities. The sequence must be non-negative and satisfy three requirements: (1) must provide an upper bound for the target density for all x in the domain, (2) must be possible to sample exactly from, and (3) must converge towards the target density as the number of support points goes to infinity. Satisfying these three criteria can be challenging, especially in the multivariate case. (Martino et al., 2018b, Section 4.2).

In the case of weighted distributions of the form (1), direct sampling as originally proposed by Walker et al. (2011) offers an appealing alternative to rejection sampling. This approach changes the formulation of the sampler to focus on the joint distribution of the target and an auxiliary variable. Sampling sequentially from the marginal density of the auxiliary variable—which is monotonically nonincreasing with support on the unit interval—and the conditional density given the auxiliary variable may be more tractable than sampling from the original target distribution. Raim (2023) utilizes a step function with the direct sampling approach to approximate the distribution of the auxiliary variable to a desired tolerance. Furthermore, the step function may be used as an envelope for rejection sampling to obtain an exact sample. One challenge that arises with the direct sampling approach is that the distribution of the latent variable may be focused on an extremely narrow interval. Computations must be sensitive to large variations in magnitude. The methods in the present paper can be used in many of the same scenarios as the direct sampler from Raim

(2023) and are more straightforward to implement.

In this paper, we introduce an adaptive rejection sampler for weighted densities, which uses vertical weighted strips (VWS) as an extension of vertical strips to form the proposal density. The VWS method utilizes decomposition (1) of the target density as a weighted form; this provides flexibility to construct efficient proposal distributions which are also convenient for use in a rejection sampler. The method is based on finding an appropriate majorizer function—i.e., one which serves as an upper bound—for the weight function. We present two variations: one is a constant function on each subset in a partition of the support and the other uses linearity to bound a weight function which is either log-convex or log-concave on each subset. Both approaches are seen to obtain practical samplers in several illustrations, with the linear majorizer achieving higher efficiency but requiring a conjugacy between the majorizer and the base distribution to be practical. Note that the VWS approach does not require that the target density itself is log-concave as in the original ARS algorithm. The direct sampling approach taken in Raim (2023) may be regarded as an application of VWS where a step function is taken as a majorizer for the density of the auxiliary random variable. Indeed, several of the theoretical results given in the present paper—along with arguments used in their proofs—are quite similar to those in Raim (2023).

The rest of this paper is organized as follows. Section 2 reviews rejection sampling and introduces VWS as a method to construct proposals. Section 3 discusses considerations in the design of a VWS proposal. Illustrations in Sections 4 and Section 5 highlight the use VWS in settings involving the von Mises Fisher distribution and Gaussian processes, respectively. Section 6 gives concluding remarks. Codes for the illustrations in Sections 4 and 5 are implemented in R (R Core Team, 2023).

2 Vertical Weighted Strips

To generate draws from target f in (1), rejection sampling requires a proposal density $h(x) = h_0(x)/\psi_*$, where $\psi_* = \int_{\Omega_n} h_0(x)d\nu(x)$, and a ratio adjustment factor M such that

$$\sup_{x \in \Omega} f_0(x)/h_0(x) \leq M. \quad (2)$$

A proposal consisting of variates u and x is generated from $\text{Uniform}(0, 1)$ and h , respectively. The proposed x is accepted as a draw from f if $u \leq f_0(x)/\{M \cdot h_0(x)\}$; otherwise, the process is repeated by redrawing u and x . This procedure may be repeated n times to obtain an independent and identically distributed sample x_1, \dots, x_n from f . A desirable choice of h is one whose support contains Ω , where h_0 is easy to evaluate, which is easy to draw variates from, and whose density is distributed in a manner not too different than f . With this formulation, it is routine to show that the probability of accepting a proposed x with accompanying u is

$$\mathbb{P}\left(U \leq \frac{f_0(X)}{Mh_0(X)}\right) = \frac{\psi}{M\psi_*}, \quad (3)$$

where $X \sim h$ and $U \sim \text{Uniform}(0, 1)$, and the distribution of an accepted draw is indeed the target distribution; i.e.,

$$\mathbb{P}\left(X \in A \mid U \leq \frac{f_0(X)}{Mh_0(X)}\right) = \int_A f(x)d\nu(x),$$

where A is a measurable set in Ω . Let S_i be the number of draws to accept the i th variate for $i = 1, \dots, n$; $\sum_{i=1}^n S_i$ is a Negative Binomial random variable with probability of success $\psi/(M\psi_*)$ and expected value $nM\psi_*/\psi$. It is apparent that the efficiency of a rejection sampler depends on the ratio of normalizing constants ψ/ψ_* and the adjustment factor M . Improvements to efficiency may be possible when h is parameterized by, say, $\boldsymbol{\vartheta}$, so that M can be minimized over $\boldsymbol{\vartheta}$:

$$\inf_{\boldsymbol{\vartheta}} \left\{ \sup_{x \in \Omega} f_0(x)/h_0(x \mid \boldsymbol{\vartheta}) \right\} \leq M.$$

Taking weighted distribution $f(x) \propto w(x)g(x)$ as the target, (2) suggests a particular class of proposals of the form

$$h(x) = h_0(x)/\psi_*, \quad h_0(x) = \bar{w}(x)g(x), \quad \psi_* = \int_{\Omega} h_0(x)d\nu(x)$$

for some function \bar{w} which majorizes the weight function w ; that is, $\bar{w}(x) \geq w(x)$ for all $x \in \Omega$. By this construction, $f_0(x) \leq h_0(x)$ for all $x \in \Omega$ so that the adjustment ratio M may be taken to be 1. We may anticipate that the rejection rate $1 - \psi/\psi_*$ will be lower when \bar{w} is close to w . However, we must also be able to readily generate variates from the resulting distribution $h_0(x)$ for it to be useful as a proposal. It may also be desirable to refine \bar{w} to be closer to w , perhaps at the cost of additional computation and/or labor by the practitioner.

In particular, consider partitioning Ω into N disjoint regions $\mathcal{D}_1, \dots, \mathcal{D}_N$, and suppose there are corresponding functions \bar{w}_j such that $\bar{w}_j(x) \geq w(x)$ for all $x \in \mathcal{D}_j$ and each region $j = 1, \dots, N$. The choice of majorizer $\bar{w}(x) = \sum_{j=1}^N \bar{w}_j(x) \mathbf{I}(x \in \mathcal{D}_j)$ yields $h_0(x) = g(x) \sum_{j=1}^N \bar{w}_j(x) \mathbf{I}(x \in \mathcal{D}_j)$. Define $\bar{\xi}_j = \mathbb{E}[\bar{w}_j(T) \mathbf{I}(T \in \mathcal{D}_j)]$ for $T \sim g$ and let $\psi_N = \sum_{j=1}^N \bar{\xi}_j$. The normalized proposal h is a finite mixture

$$\begin{aligned} h(x) &= h_0(x)/\psi_N \\ &= \sum_{j=1}^N \frac{\bar{\xi}_j}{\sum_{\ell=1}^N \bar{\xi}_\ell} \bar{w}_j(x)g(x) \mathbf{I}(x \in \mathcal{D}_j)/\bar{\xi}_j \\ &= \sum_{j=1}^N \pi_j g_j(x), \end{aligned}$$

whose component densities $g_j(x) = \bar{w}_j(x)g(x) \mathbf{I}(x \in \mathcal{D}_j)/\bar{\xi}_j$ are truncated and reweighted versions of base distribution g and whose mixing weights are $\pi_j = \bar{\xi}_j/\{\sum_{\ell=1}^N \bar{\xi}_\ell\}$. The dependence on N in the notation ψ_N is emphasized for the upcoming discussion, but it is understood that other terms in the formulation of the proposal depend on N as well. We refer to the rejection sampling method with proposal h as vertical weighted strips. Generating a variate from h can be accomplished using its finite mixture formulation by drawing index j from a discrete distribution on values $1, \dots, N$ with probabilities π_1, \dots, π_N , then drawing x from the truncated base distribution g_j .

From (3), the probability that a draw from a VWS proposal is rejected is $1 - \psi/\psi_N$. A value of this probability which is nearly 1 results in a rejection sampler which accepts so rarely as to be unusable. With insight into this probability, a practitioner can take actions such as adapting $\mathcal{D}_1, \dots, \mathcal{D}_N$ into a finer partition, refactoring the weight/base decomposition, or considering different classes of majorizers for \bar{w}_j . When the normalizing constant ψ is intractable, an upper bound for $1 - \psi/\psi_N$ can be considered instead. Suppose \underline{w}_j is a minorizing function of w so that $0 \leq \underline{w}_j(x) \leq w(x)$ for all $x \in \mathcal{D}_j$, $j = 1, \dots, N$, and let $\underline{\xi}_j = \mathbb{E}[\underline{w}_j(T) \mathbf{I}(T \in \mathcal{D}_j)]$ where $T \sim g$. The following is straightforward to prove, but is stated as result because of its utility.

Proposition 1. *Under VWS, the probability (3) of a proposed draw being rejected is bounded above by*

$$1 - \frac{\sum_{j=1}^N \underline{\xi}_j}{\sum_{j=1}^N \bar{\xi}_j}. \quad (4)$$

Proof. The true rejection probability is

$$\begin{aligned}
\frac{\psi_N - \psi}{\psi_N} &= \frac{1}{\psi_N} \int_{\Omega} [h_0(x) - f_0(x)] d\nu(x) \\
&= \frac{1}{\psi_N} \sum_{j=1}^N \int_{\Omega} \mathbf{I}(x \in \mathcal{D}_j) [\bar{w}_j(x) - w(x)] g(x) d\nu(x) \\
&\leq \frac{1}{\psi_N} \sum_{j=1}^N \int_{\Omega} \mathbf{I}(x \in \mathcal{D}_j) [\bar{w}_j(x) - \underline{w}_j(x)] g(x) d\nu(x) \\
&= \frac{1}{\psi_N} \left\{ \sum_{j=1}^N \bar{\xi}_j - \sum_{j=1}^N \underline{\xi}_j \right\},
\end{aligned}$$

which is equivalent to (4). \square

Remark 1. When integrals $\underline{\xi}_j = \int_{\mathcal{D}_j} \underline{w}_j(x) g(x) d\nu(x)$ are tractable using the trivial minorizer $\underline{w}_j(x) = w(x) \cdot \mathbf{I}(x \in \mathcal{D}_j)$, the bound (4) is equivalent to the actual rejection probability $1 - \psi/\psi_N$.

The rejection probability $1 - \psi/\psi_N$ may also be interpreted as a relative error in approximating the normalizing constant ψ by the normalizing constant ψ_N . If the distribution h can be designed in such a way that this relative error is small, the following result shows that probabilities computed under the proposal will be close to probabilities computed under the target. This suggests another way that h may be useful as an approximation to f , aside from rejection sampling.

Proposition 2. Let \mathcal{B} denote the collection of measurable subsets of Ω , $X \sim f$, and $\tilde{X} \sim h$; then

$$\sup_{B \in \mathcal{B}} \left| \mathbb{P}(\tilde{X} \in B) - \mathbb{P}(X \in B) \right| \leq \frac{\psi_N - \psi}{\psi_N}. \quad (5)$$

Proof. For any $B \in \mathcal{B}$,

$$\begin{aligned}
\int_B h(x) d\nu(x) - \int_B f(x) d\nu(x) &= \frac{1}{\psi_N} \int_B h_0(x) d\nu(x) - \frac{1}{\psi} \int_B f_0(x) d\nu(x) \\
&\leq \frac{1}{\psi_N} \left[\int_B h_0(x) d\nu(x) - \int_B f_0(x) d\nu(x) \right] \\
&= \frac{1}{\psi_N} \sum_{j=1}^N \int_{B \cap \mathcal{D}_j} [\bar{w}_j(x) - w(x)] g(x) d\nu(x) \\
&\leq \frac{1}{\psi_N} \sum_{j=1}^N \int_{\mathcal{D}_j} [\bar{w}_j(x) - w(x)] g(x) d\nu(x) \\
&= \frac{\psi_N - \psi}{\psi_N}
\end{aligned} \quad (6)$$

and

$$\begin{aligned}
\int_B f(x) d\nu(x) - \int_B h(x) d\nu(x) &= \frac{1}{\psi} \int_B f_0(x) d\nu(x) - \frac{1}{\psi_N} \int_B h_0(x) d\nu(x) \\
&\leq \frac{1}{\psi} \int_B f_0(x) d\nu(x) - \frac{1}{\psi_N} \int_B f_0(x) d\nu(x) \\
&= \frac{\psi_N - \psi}{\psi_N} \int_B f(x) d\nu(x) \\
&\leq \frac{\psi_N - \psi}{\psi_N}.
\end{aligned} \quad (7)$$

Combining (6) and (7) gives the result. \square

The remainder of the paper will focus on the case where f is a univariate target. Here, Ω is a subset of the real line, and we will further assume that regions \mathcal{D}_j take the form of intervals $(\alpha_{j-1}, \alpha_j]$ for $j = 1, \dots, N$. Here, the process of sampling from h can be handled in a similar way across many univariate problems. The cumulative distribution function (CDF) associated with proposal distribution h may be written as

$$H(x) = \sum_{j=1}^{\ell-1} \pi_j + \pi_\ell G_\ell(x), \quad G_\ell(x) = \frac{\int_{(\alpha_{\ell-1}, x]} \bar{w}_\ell(s) g(s) d\nu(s)}{\int_{(\alpha_{\ell-1}, \alpha_\ell]} \bar{w}_\ell(s) g(s) d\nu(s)}, \quad \text{if } x \in (\alpha_{\ell-1}, \alpha_\ell].$$

To obtain the quantile function, suppose $\varphi \in [0, 1]$ and ℓ is the index such that $\sum_{j=1}^{\ell-1} \pi_j < \varphi \leq \sum_{j=1}^{\ell} \pi_j$; then

$$\varphi \leq H(x) \equiv \sum_{j=1}^{\ell-1} \pi_j + \pi_\ell G_\ell(x) \iff G_\ell(x) \geq \frac{\varphi - \sum_{j=1}^{\ell-1} \pi_j}{\pi_\ell} = \frac{1}{\bar{\xi}_\ell} \left[\varphi \sum_{j=1}^N \bar{\xi}_j - \sum_{j=1}^{\ell-1} \bar{\xi}_j \right]. \quad (8)$$

Therefore, the quantile function associated with H is

$$\begin{aligned} H^-(\varphi) &= \inf\{x \in \Omega : H(x) \geq \varphi\} \\ &= \inf \left\{ x \in \Omega : G_\ell(x) \geq \frac{1}{\bar{\xi}_\ell} \left[\varphi \sum_{j=1}^N \bar{\xi}_j - \sum_{j=1}^{\ell-1} \bar{\xi}_j \right] \right\} \\ &= G_\ell^- \left(\frac{1}{\bar{\xi}_\ell} \left[\varphi \sum_{j=1}^N \bar{\xi}_j - \sum_{j=1}^{\ell-1} \bar{\xi}_j \right] \right), \end{aligned} \quad (9)$$

where G_ℓ^- is the quantile function associated with base distribution g . Computations involving H and H^- can be facilitated by precomputing the cumulative sums $H(x_\ell) = \sum_{j=1}^{\ell} \pi_j$ for $\ell = 1, \dots, N$. Then, for example, a binary search can be carried out to find the smallest ℓ such that $H(x_\ell) \geq \varphi$. Variates from h can be generated with the inverse CDF method as $x = H^-(u)$ where u is a draw from $\text{Uniform}(0, 1)$.

3 Design of Proposal

The VWS proposal was introduced as a finite mixture of reweighted and truncated versions of the base distribution g on the partition $\mathcal{D}_1, \dots, \mathcal{D}_N$, but we have not yet discussed choices in determining \mathcal{D}_j or \bar{w}_j which are crucial to the method. It is unsurprising to first note that if $\bar{w}_j(x) \approx w(x)$ for all $x \in \mathcal{D}_j$ and each $j = 1, \dots, N$, then $1 - \psi/\psi_N \approx 0$ so that rejection sampling practically always accepts. However, it is also desirable to create a relatively small number of regions N , especially avoiding regions which do not substantially contribute to the approximation. An efficient implementation of the sampler must consider computation of $\bar{\xi}_j$ for mixture weights, and generating draws from the g_j densities should be significantly easier than the original f .

3.1 Factorization

The weight function and base distribution in (1) are not unique. For any function $q(x)$ which is positive on Ω ,

$$f_0(x) = w(x) \frac{1}{q(x)} \cdot q(x) g(x) = \tilde{w}(x) \tilde{g}(x),$$

where $\tilde{w}(x) = w(x)/q(x)$ and $\tilde{g}(x) = q(x)g(x)$. The choice of a suitable q —which is often utilized in importance sampling (Robert and Casella, 2004, e.g., Chapter 3)—can be leveraged in VWS. We may select

q to facilitate majorization of w and to facilitate operations with truncated and reweighted g . One situation which can sometimes be avoided by such a refactorizing occurs when the density of g is far removed from that of f so that the distributions are practically on disjoint subsets of Ω ; numerical issues may arise in this situation due to the very small probabilities involved.

Remark 2 (Vertical Strips). When the support Ω is bounded, the standard vertical strips (VS) method is a special case of VWS with $w(x) = f_0(x)$ and g taken to be the uniform distribution on Ω . The proposal

$$h(x) = \sum_{j=1}^N \pi_j g_j(x), \quad \pi_j = \frac{\bar{\xi}_j}{\sum_{\ell=1}^N \bar{\xi}_\ell}, \quad g_j(x) = \frac{\mathbf{I}(x \in \mathcal{D}_j)}{\int_{\mathcal{D}_j} du},$$

is a finite mixture of Uniform distributions with $\bar{\xi}_j = \bar{f}_{0j} \cdot \int_{\mathcal{D}_j} du$ and $\bar{f}_{0j} = \max_{x \in \mathcal{D}_j} f_0(x)$. The minorizer $\underline{f}_{0j} = \min_{x \in \mathcal{D}_j} f_0(x)$ may be used to form the bound (4). The respective optimizations may be carried out numerically in the absence of closed-form solutions.

By utilizing a decomposition of the target into a weight function and base density, it may be possible to obtain a more efficient sampler. Sections 3.2 and 3.3 describe the use of a constant function and linear function, respectively, in the majorizer and minorizer.

3.2 Constant Majorizer

When $w_j(x) < \infty$ for $x \in \mathcal{D}_j$, a choice of $\bar{w}_j(x)$ is the constant $\bar{w}_j = \sup_{x \in \mathcal{D}_j} w(x)$ for $j = 1, \dots, N$. Similarly, the minorizer may be taken as $\underline{w}_j = \inf_{x \in \mathcal{D}_j} w(x)$. Here the proposal density becomes

$$h(x) = \sum_{j=1}^N \pi_j g_j(x), \quad \pi_j = \frac{\bar{\xi}_j}{\sum_{\ell=1}^N \bar{\xi}_\ell}, \quad g_j(x) = \frac{g(x) \mathbf{I}(x \in \mathcal{D}_j)}{\mathbf{P}(T \in \mathcal{D}_j)},$$

where $\bar{\xi}_j = \bar{w}_j \mathbf{P}(T \in \mathcal{D}_j)$ and $T \sim g$. Here the g_j represent the base distribution $g(x)$ truncated to the set \mathcal{D}_j so that reweighting is avoided. The minorizer $\underline{w}_j = \min_{x \in \mathcal{D}_j} w_j(x)$ may be used to form the bound (4).

In this case, the CDF of the proposal simplifies to

$$G_\ell(x) = \frac{G(x) - G(\alpha_{\ell-1})}{G(\alpha_\ell) - G(\alpha_{\ell-1})}, \quad \text{if } x \in (\alpha_{\ell-1}, \alpha_\ell]$$

and (8) simplifies to

$$\begin{aligned} G_\ell(x) &\geq \frac{1}{\bar{\xi}_\ell} \left[\varphi \sum_{j=1}^N \bar{\xi}_j - \sum_{j=1}^{\ell-1} \bar{\xi}_j \right] \\ \iff \frac{G(x) - G(\alpha_{\ell-1})}{G(\alpha_\ell) - G(\alpha_{\ell-1})} &\geq \frac{\varphi \sum_{j=1}^N \bar{w}_j [G(\alpha_j) - G(\alpha_{j-1})] - \sum_{j=1}^{\ell-1} \bar{w}_j [G(\alpha_j) - G(\alpha_{j-1})]}{\bar{w}_\ell [G(\alpha_\ell) - G(\alpha_{\ell-1})]} \\ \iff G(x) &\geq G(\alpha_{\ell-1}) + \frac{1}{\bar{w}_\ell} \left[\varphi \sum_{j=1}^N \bar{w}_j [G(\alpha_j) - G(\alpha_{j-1})] - \sum_{j=1}^{\ell-1} \bar{w}_j [G(\alpha_j) - G(\alpha_{j-1})] \right]. \end{aligned} \quad (10)$$

Combining (10) with (9), the quantile of the original base distribution g specified by the expression on the right-hand side of (10) coincides with the φ quantile of H . With numerical optimization and the inverse CDF method, use of the constant majorizer and minorizer lends itself to flexible VWS code in the univariate setting which can handle many choices of w and g .

3.3 Linear Majorizer

Suppose it is possible to partition Ω into regions \mathcal{D}_j where w is either a log-convex or log-concave function. Here we can use linear functions to majorize / minorize w and potentially gain improved accuracy over VS and VWS with constant functions. Suppose $w(x)$ is finite and log-concave on $\mathcal{D}_j = (\alpha_{j-1}, \alpha_j]$; then for $c \in \mathcal{D}_j$,

$$\begin{aligned} \log w(x) &\leq \log w(c) + (x - c)\nabla(c), \\ &= \bar{\beta}_{j0} + \bar{\beta}_{j1} \cdot x \end{aligned} \quad (11)$$

where $\bar{\beta}_{j0} = \log w_j(c) - c \cdot \nabla(c)$, $\bar{\beta}_{j1} = \nabla(c)$, and $\nabla(x) = \frac{d}{dx} \log w(x)$. Therefore, the function $\bar{w}_j(x) = \exp\{\bar{\beta}_{j0} + \bar{\beta}_{j1} \cdot x\}$ is majorizer for $w(x)$ on \mathcal{D}_j . Note that the constant term $\exp\{\bar{\beta}_{j0}\}$ cancels from the density g_j upon normalization but is needed in formulating $\bar{\xi}_j$ so that the unnormalized h_0 majorizes f_0 . The expansion point c may be chosen to yield a small upper bound (11) over all $x \in \mathcal{D}_j$. A criteria to select c —which will be utilized in this work—is to minimize the L1 distance between unnormalized densities h_0 and f_0 on \mathcal{D}_j ,

$$\begin{aligned} c^* &= \operatorname{argmin}_{c \in \mathcal{D}_j} \int_{\mathcal{D}_j} |h_0(x) - f_0(x)| d\nu(x) \\ &= \operatorname{argmin}_{c \in \mathcal{D}_j} \int_{\mathcal{D}_j} [\bar{w}_j(x) - w(x)] g(x) d\nu(x) \\ &= \operatorname{argmin}_{c \in \mathcal{D}_j} \left\{ w(c) \exp\{-c\nabla(c)\} \int_{\mathcal{D}_j} \exp\{x\nabla(c)\} g(x) d\nu(x) \right\} \\ &= \operatorname{argmin}_{c \in \mathcal{D}_j} \left\{ w(c) \exp\{-c\nabla(c)\} \mathbb{P}(T \in \mathcal{D}_j) M_j(\nabla(c)) \right\} \\ &= \operatorname{argmin}_{c \in \mathcal{D}_j} \left\{ \log w(c) - c\nabla(c) + \log M_j(\nabla(c)) \right\}, \end{aligned} \quad (12)$$

where $M_j(s)$ is the moment generating function of random variable $T \cdot \mathbb{I}\{\alpha_{j-1} < T \leq \alpha_j\}$.

To obtain a minorizer, x may be expressed as a convex combination of the endpoints $\{\alpha_{j-1}, \alpha_j\}$ as $x = (1 - \lambda)\alpha_{j-1} + \lambda\alpha_j$ so that $\lambda = (x - \alpha_{j-1})/(\alpha_j - \alpha_{j-1})$. Concavity of $\log w(x)$ gives

$$\begin{aligned} \log w(x) &\geq (1 - \lambda) \log w(\alpha_{j-1}) + \lambda \log w(\alpha_j) \\ &= \log w(\alpha_{j-1}) + \frac{x - \alpha_{j-1}}{\alpha_j - \alpha_{j-1}} [\log w(\alpha_j) - \log w(\alpha_{j-1})] \\ &= \underline{\beta}_{j0} + \underline{\beta}_{j1} \cdot x, \end{aligned} \quad (13)$$

with $\underline{\beta}_{j0} = \log w(\alpha_{j-1}) - \alpha_{j-1}\underline{\beta}_{j1}$ and $\underline{\beta}_{j1} = \{\log w(\alpha_j) - \log w(\alpha_{j-1})\}/\{\alpha_j - \alpha_{j-1}\}$, so that the function $\underline{w}(x) = \exp\{\underline{\beta}_{j0} + \underline{\beta}_{j1} \cdot x\}$ is minorizer for $w(x)$ on \mathcal{D}_j . In the case that w is log-convex rather than log-concave, the majorizer and minorizer in (11) and (13) switch roles. Similar to (12), a choice of c for the minorizer can be obtained from

$$\begin{aligned} c^* &= \operatorname{argmin}_{c \in \mathcal{D}_j} \int_{\mathcal{D}_j} [w(x) - \underline{w}_j(x)] g(x) d\nu(x) \\ &= \operatorname{argmax}_{c \in \mathcal{D}_j} \int_{\mathcal{D}_j} \underline{w}_j(x) g(x) d\nu(x) \\ &= \operatorname{argmax}_{c \in \mathcal{D}_j} \left\{ \log w(c) - c\nabla(c) + \log M_j(\nabla(c)) \right\}. \end{aligned} \quad (14)$$

The following examples present cases where a linear majorizer and minorizer yield practical proposals in Sections 4 and 5.

Example 1 (Exponential Family Base with Linear Majorizer). Suppose w_j is log-convex or log-concave and base distribution g has exponential family density $g(x) = \exp\{\vartheta x - a(\vartheta)\}$ with respect to dominating measure $\nu(x)$ and $\vartheta \in \mathbb{R}$. Equation (11) gives majorizer

$$\bar{\xi}_j = \int_{\mathcal{D}_j} \bar{w}_j(x)g(x)d\nu(x) = \exp(\bar{\beta}_{j0}) \int_{\mathcal{D}_j} \exp\{(\bar{\beta}_{j1} + \vartheta)x - a(\vartheta)\}d\nu(x),$$

and similarly (13) gives minorizer

$$\underline{\xi}_j = \int_{\mathcal{D}_j} \underline{w}_j(x)g(x)d\nu(x) = \exp(\underline{\beta}_{j0}) \int_{\mathcal{D}_j} \exp\{(\underline{\beta}_{j1} + \vartheta)x - a(\vartheta)\}d\nu(x).$$

Here, the proposal mixture component

$$\begin{aligned} g_j(x) &= \bar{w}_j(x)g(x)\mathbf{I}(x \in \mathcal{D}_j)/\bar{\xi}_j \\ &= \frac{\exp\{(\bar{\beta}_{j1} + \vartheta)x - a(\vartheta)\}\mathbf{I}(x \in \mathcal{D}_j)}{\int_{\mathcal{D}_j} \exp\{(\bar{\beta}_{j1} + \vartheta)s - a(\vartheta)\}d\nu(s)} \end{aligned}$$

is a member of the same family as g , but truncated to the interval $(\alpha_{j-1}, \alpha_j]$.

Example 2 (Doubly-Truncated Exponential Base with Linear Majorizer). Let $X \sim \text{Exp}_{(a,b)}(\kappa)$ denote a random variable with doubly truncated exponential distribution whose density is

$$g(x) = \frac{\kappa e^{\kappa x}}{e^{\kappa b} - e^{\kappa a}} \cdot \mathbf{I}(a < x < b),$$

where $-\infty < a < b < \infty$ and κ may be any real number. Draws from $\text{Exp}_{(a,b)}(\kappa)$ may be generated with the inverse CDF method, where the CDF and associated quantile function are, respectively,

$$G(x) = \frac{e^{\kappa x} - e^{\kappa a}}{e^{\kappa b} - e^{\kappa a}}, \quad x \in (a, b), \quad (15)$$

$$G^{-1}(\varphi) = \frac{1}{\kappa} \log [e^{\kappa a} + \varphi(e^{\kappa b} - e^{\kappa a})], \quad \varphi \in [0, 1]. \quad (16)$$

Consider using g as a base distribution with majorizer (11) and minorizer (13); expressions obtained in Example 1 for exponential families give

$$\begin{aligned} \bar{\xi}_j &= \frac{\kappa \exp\{\bar{\beta}_{j0}\}}{(\kappa + \bar{\beta}_{j1})(e^\kappa - e^{-\kappa})} \left\{ \exp\{(\kappa + \bar{\beta}_{j1})\alpha_j\} - \exp\{(\kappa + \bar{\beta}_{j1})\alpha_{j-1}\} \right\}, \\ \underline{\xi}_j &= \frac{\kappa \exp\{\underline{\beta}_{j0}\}}{(\kappa + \underline{\beta}_{j1})(e^\kappa - e^{-\kappa})} \left\{ \exp\{(\kappa + \underline{\beta}_{j1})\alpha_j\} - \exp\{(\kappa + \underline{\beta}_{j1})\alpha_{j-1}\} \right\}. \end{aligned}$$

The reweighted and truncated distribution for the j th mixture component of finite mixture h is

$$g_j(x) = \frac{(\kappa + \bar{\beta}_{j1}) \exp\{(\kappa + \bar{\beta}_{j1})x\}}{\exp\{(\kappa + \bar{\beta}_{j1})\alpha_j\} - \exp\{(\kappa + \bar{\beta}_{j1})\alpha_{j-1}\}} \cdot \mathbf{I}(\alpha_{j-1} < x \leq \alpha_j).$$

The moment generating function utilized in (12) and (14) is

$$M_j(s) = \int_a^b \frac{e^{xs}g(x)\mathbf{I}(\alpha_{j-1} < x \leq \alpha_j)}{\mathbf{P}(\alpha_{j-1} < T \leq \alpha_j)} dx = \frac{\kappa}{s + \kappa} \frac{e^{(s+\kappa)\alpha_j} - e^{(s+\kappa)\alpha_{j-1}}}{e^{\kappa\alpha_j} - e^{\kappa\alpha_{j-1}}}.$$

Example 3 (Uniform Base with Linear Majorizer). Suppose w_j is log-convex or log-concave and base distribution g has uniform density $g(x) = \mathbb{I}(x \in [a, b]) / (b - a)$ so that $\Omega = [a, b]$ is also the support of the target. Majorizer (11) and minorizer (13) give, respectively,

$$\begin{aligned}\bar{\xi}_j &= \int_{\mathcal{D}_j} \exp\{\bar{\beta}_{j0} + \bar{\beta}_{j1}x\} d\nu(x) = \frac{\exp\{\bar{\beta}_{j0}\}}{(b-a)\bar{\beta}_{j1}} \left(\exp\{\bar{\beta}_{j1} \cdot \alpha_j\} - \exp\{\bar{\beta}_{j1} \cdot \alpha_{j-1}\} \right), \\ \underline{\xi}_j &= \int_{\mathcal{D}_j} \exp\{\underline{\beta}_{j0} + \underline{\beta}_{j1}x\} d\nu(x) = \frac{\exp\{\underline{\beta}_{j0}\}}{(b-a)\underline{\beta}_{j1}} \left(\exp\{\underline{\beta}_{j1} \cdot \alpha_j\} - \exp\{\underline{\beta}_{j1} \cdot \alpha_{j-1}\} \right).\end{aligned}$$

The j th proposal mixture component becomes

$$g_j(x) = \frac{\bar{\beta}_{j1} \cdot \exp\{\bar{\beta}_{j1} \cdot x\}}{\exp\{\bar{\beta}_{j1} \cdot \alpha_j\} - \exp\{\bar{\beta}_{j1} \cdot \alpha_{j-1}\}} \mathbb{I}(\alpha_{j-1} < x \leq \alpha_j)$$

so that a random variable T with density g_j is distributed as $\text{Exp}_{(\alpha_{j-1}, \alpha_j]}(\bar{\beta}_{j1})$, similarly to Example 2. The moment generating function utilized in (12) and (14) is

$$M_j(s) = \frac{e^{s\alpha_j} - e^{s\alpha_{j-1}}}{s(\alpha_j - \alpha_{j-1})}.$$

Remark 3. It is not required to use a common factorization across all regions $\mathcal{D}_1, \dots, \mathcal{D}_N$; it may be useful to mix and match, at the expense of extra bookkeeping by the practitioner. Suppose we have formulated a proposal using the constant or linear approaches, but $\sup_{x \in \mathcal{D}_j} w(x) = \infty$ for some j . We may opt to use a different factorization in this region. For example, if f_0 is finite on \mathcal{D}_j , the VS method may be used here. In this paper, there are several situations where $w(x) \rightarrow \infty$ as x approaches the upper or lower limits of the support $(\alpha_0, \alpha_N]$. We have taken a simpler approach and truncated the support to $(\alpha_0 + \epsilon, \alpha_N - \epsilon]$ for a small $\epsilon > 0$.

3.4 Knot Selection

An important consideration in achieving a satisfactory acceptance rate is the method of selecting knots $\alpha_1, \dots, \alpha_{N-1}$ which partition the domain Ω into regions $\mathcal{D}_j = (\alpha_{j-1}, \alpha_j]$ for $j = 1, \dots, N$. It is desirable that the rejection rate $1 - \psi/\psi_N$ reduces rapidly as N increases. If a very large N is required, the effort to prepare the proposal and draw variates may not be worth the efficiency achieved in the final sampler. Strategies involving equally spaced intervals and producing regions with equal probabilities have been considered by Hörmann (2002). In this work, we consider a rule of thumb which seeks to reduce upper bound $\sum_{\ell=1}^N \{\bar{\xi}_\ell - \underline{\xi}_\ell\} / \{\sum_{j=1}^N \bar{\xi}_j\}$ from (4). With N regions in the partition, the contribution of the ℓ th region to the upper bound can be characterized as

$$\rho_\ell = \frac{\bar{\xi}_\ell - \underline{\xi}_\ell}{\sum_{j=1}^N \bar{\xi}_j}, \quad (17)$$

so that ρ_1, \dots, ρ_N sum to (4). A region to split is selected by drawing index ℓ^* from the discrete distribution on $1, \dots, N$ with probabilities proportional to ρ_1, \dots, ρ_N . This amounts to a greedy selection to reduce the bound, but with an opportunity for all regions to be selected with positive probability. The region ℓ^* is then bifurcated in a prescribed way so that region $\mathcal{D}_\ell = (\alpha_{\ell-1}, \alpha_\ell]$ is replaced with $\mathcal{D}_\ell^{(1)} = (\alpha_{\ell-1}, \alpha_{\ell^*}]$ and $\mathcal{D}_\ell^{(2)} = (\alpha_{\ell^*}, \alpha_\ell]$. In this work, we use

$$\alpha_{\ell^*} = \begin{cases} 0 & \text{if } \alpha_{\ell-1} = -\infty \text{ and } \alpha_\ell = \infty, \\ \alpha_\ell - |\alpha_\ell| - 1 & \text{if } \alpha_{\ell-1} = -\infty \text{ and } \alpha_\ell < \infty, \\ \alpha_{\ell-1} + |\alpha_{\ell-1}| + 1 & \text{if } \alpha_{\ell-1} > -\infty \text{ and } \alpha_\ell = \infty, \\ (\alpha_{\ell-1} + \alpha_\ell)/2 & \text{otherwise.} \end{cases}$$

when the target is a continuous distribution; i.e., the arithmetic midpoint when both endpoints are finite and zero when both are infinite. When one of the two is finite, α_{ℓ^*} is taken to be a shifted version of it. A similar bifurcation is used when the target is a discrete distribution, but with $\alpha_{\ell^*} = \lceil(\alpha_{\ell-1} + \alpha_{\ell})/2\rceil$ in the case that both endpoints are finite. If no values from the support are within $(\alpha_{\ell-1}, \alpha_{\ell}]$, the region should be excluded from further bifurcation; this follows from $\rho_{\ell} = 0$. It is also possible to use a rejected draw x to adapt the proposal during sampling; for example, by identifying the region \mathcal{D}_{ℓ^*} which contains x and splitting it at x . In this work, however, we have opted to partition entirely before sampling.

4 Illustrations with von Mises Fisher Distribution

The von Mises Fisher (VMF) distribution provides several opportunities to illustrate the vertical weighted strips approach. VMF arises in the study of directional data which are observed on the d -dimensional sphere $\mathbb{S}^d = \{\mathbf{v} \in \mathbb{R}^d : \mathbf{v}^\top \mathbf{v} = 1\}$. Fisher et al. (1993) and Mardia and Jupp (1999) give comprehensive treatments in this area and Pewsey and García-Portugués (2021) provides a survey of more recent developments. A random variable \mathbf{V} with distribution $\text{VMF}_d(\boldsymbol{\mu}, \kappa)$ has density

$$f_{\text{VMF}}(\mathbf{v}) = \frac{\kappa^{d/2-1}}{(2\pi)^{-d/2} I_{d/2-1}(\kappa)} \exp(\kappa \cdot \boldsymbol{\mu}^\top \mathbf{v}) \cdot \mathbf{I}(\mathbf{v} \in \mathbb{S}^d),$$

with modified Bessel function of the first kind $I_\nu(x) = \sum_{m=0}^{\infty} \{m! \cdot \Gamma(m + \nu + 1)\}^{-1} (\frac{x}{2})^{2m+\nu}$. Parameter $\boldsymbol{\mu} \in \mathbb{S}^d$ determines the direction of the mode and parameter $\kappa > 0$ determines the concentration. This section will consider the VWS approach in three von Mises Fisher scenarios. Section 4.1 demonstrates variate generation from VMF. Section 4.2 uses a VWS proposal to approximately compute probabilities—without Monte Carlo—via Proposition 2. Section 4.3 presents a Bayesian application with independent and identically distributed VMF outcomes where rejection sampling may be used in lieu of MCMC. Going forward, we will refer to the constant majorization described in Section 3.2 as “constant VWS” and the linear majorization described in Section 3.3 as “linear VWS”.

4.1 Generation of Variates

A widely used method to generate variates from $\text{VMF}_d(\boldsymbol{\mu}, \kappa)$ is a rejection sampling scheme developed by Ulrich (1984) and Wood (1994). For example, this method is used in the R packages `movMF` (Hornik and Grün, 2014) and `Rfast` (Tsagris and Papadakis, 2018). The sampler is based on the following construction. Without loss of generality, suppose $\boldsymbol{\mu}_0 = (1, 0, \dots, 0)$. A random variable $\mathbf{V}_0 \sim \text{VMF}_d(\boldsymbol{\mu}_0, \kappa)$ can be obtained using

$$\mathbf{V}_0 = \left(X, \sqrt{1 - X^2} \cdot \mathbf{U} \right), \tag{18}$$

where \mathbf{U} is a uniform random variable on the sphere \mathbb{S}^{d-1} and X has density

$$f(x) = \frac{(\kappa/2)^{d/2-1} (1 - x^2)^{(d-3)/2} \exp(\kappa x)}{\sqrt{\pi} \cdot I_{d/2-1}(\kappa) \cdot \Gamma((d-1)/2)} \cdot \mathbf{I}(-1 < x < 1). \tag{19}$$

A draw of \mathbf{U} can be readily obtained from $\mathbf{Z}/\sqrt{\mathbf{Z}^\top \mathbf{Z}}$ with $\mathbf{Z} \sim \text{N}(\mathbf{0}, \mathbf{I}_{d-1})$ (Muller, 1959). Furthermore, $\mathbf{V} \sim \text{VMF}_d(\boldsymbol{\mu}, \kappa)$ for an arbitrary $\boldsymbol{\mu}$ can be obtained from \mathbf{V}_0 using $\mathbf{V} = \mathbf{Q}\mathbf{V}_0$ with an orthonormal matrix \mathbf{Q} whose first column is $\boldsymbol{\mu}$. Therefore, the problem of drawing \mathbf{V}_0 reduces to univariate generation of X . Ulrich (1984) and Wood (1994) developed a proposal for X based on $Z \sim \text{Beta}((d-1)/2, (d-1)/2)$ via the random variable $X_0 = [1 - (1+b)Z]/[1 - (1-b)Z]$ with density

$$h_{X_0}(x | b) = \frac{2 \cdot b^{(d-1)/2} (1 - x^2)^{(d-3)/2}}{B((d-1)/2, (d-1)/2) \cdot [(1+b) - (1-b)x]^{d-1}}, \quad x \in (-1, 1), \tag{20}$$

Table 1: Rejection rates as percentage $100 \times (1 - \psi/\psi_*)$ for the simple VWS sampler.

d	κ								
	0.1	0.2	0.5	1	2	5	10	20	50
4	8.23	8.28	8.67	9.98	14.24	28.22	42.79	56.82	71.56
5	10.76	10.83	11.32	13.01	18.73	38.95	59.70	76.62	89.76
10	8.60	8.65	8.97	10.11	14.50	38.44	73.71	94.50	99.64
20	4.16	4.17	4.26	4.58	5.86	15.43	48.50	93.45	99.98
50	1.56	1.56	1.58	1.62	1.82	3.23	9.33	41.17	99.86

where $b \in (0, 1)$ is a fixed number. The smallest M such that $f(x)/\{Mh_{X_0}(x | b)\} \leq 1$ for all $x \in (-1, 1)$ is obtained from

$$x_* = \frac{1 - b_*}{1 + b_*}, \quad b_* = \frac{-2\kappa + \sqrt{4\kappa^2 + (d-1)^2}}{d-1}.$$

Let $c = \kappa x_* + (d-1) \log(1 - x_*^2)$. The rejection sampler proceeds by generating x from proposal (20) and u from Uniform(0, 1). We accept x as a draw from the target if $\log u < \kappa x + (d-1) \log(1 - x \cdot x_*) - c$; otherwise, we reject x and u and draw again. We will refer to this as the UW sampler. Before proceeding, we note an alternative approach from Kurz and Hanebeck (2015) to sample from target (19). Here, an inverse CDF method is obtained by deriving expressions for the CDF which are free of integrals, and using a bisection algorithm to numerically compute the quantile function.

As a first demonstration of the VWS approach, let us first consider a simple proposal that makes use of the inequality $1 - x^2 \leq e^{-x^2}$ without partitioning the support. For any $d > 3$, $f_0(x) = (1 - x^2)^{(d-3)/2} e^{\kappa x} \mathbf{I}(-1 < x < 1)$ is majorized by $h_0(x) = e^{-x^2(d-3)/2 + \kappa x} \mathbf{I}(-1 < x < 1)$. Stated in terms of the weighted density form, $w(x) = (1 - x^2)^{(d-3)/2}$ is majorized by $\bar{w}(x) = e^{-x^2(d-3)/2}$ and the base density g is taken to be $g(x) = e^{\kappa x} \mathbf{I}(-1 < x < 1)$. Here, the normalizing constant for target f is

$$\psi = \frac{\sqrt{\pi} \cdot I_{d/2-1}(\kappa) \cdot \Gamma((d-1)/2)}{(e^\kappa - e^{-\kappa}) \cdot (\kappa/2)^{d/2-1}},$$

which can be computed in closed form. The function h_0 is recognized as an unnormalized density for random variable $T \sim N(\kappa(d-3)^{-1}, (d-3)^{-1})$ which has been truncated to the interval $(-1, 1)$. After completing the square and adjusting for the truncated support, the normalized proposal and normalizing constant are, respectively,

$$h(x) = \sqrt{\frac{d-3}{2\pi}} \exp\left\{-\frac{d-3}{2} [x - \kappa(d-3)^{-1}]^2\right\} \cdot \frac{\mathbf{I}(-1 < x < 1)}{\mathbf{P}(-1 < T < 1)}$$

and

$$\psi_* = \sqrt{\frac{2\pi}{d-3}} \exp\left\{\frac{1}{2}\kappa(d-3)^{-1}\right\} \cdot \frac{\mathbf{I}(-1 < x < 1)}{\mathbf{P}(-1 < T < 1)}.$$

Drawing from proposal h is straightforward using the inverse CDF method; i.e., by using the quantile function in (10) with $N = 1$. We may therefore proceed with rejection sampling as usual by generating u and x from Uniform(0, 1) and h , respectively, and accepting x when $u \leq f_0(x)/h_0(x)$. Table 1 displays the rejection rate $1 - \psi/\psi_*$ for several settings of d and κ . Acceptance is relatively frequent for smaller κ but the sampler becomes increasingly inefficient as κ increases beyond 1. It is interesting to note that rejection rate does not increase monotonically with d . Figure 1 compares the proposal and target for the case $\kappa = 10$ and $d = 10$; it is apparent that h_0 is not an efficient majorizer for f_0 as x increases beyond 0.5.

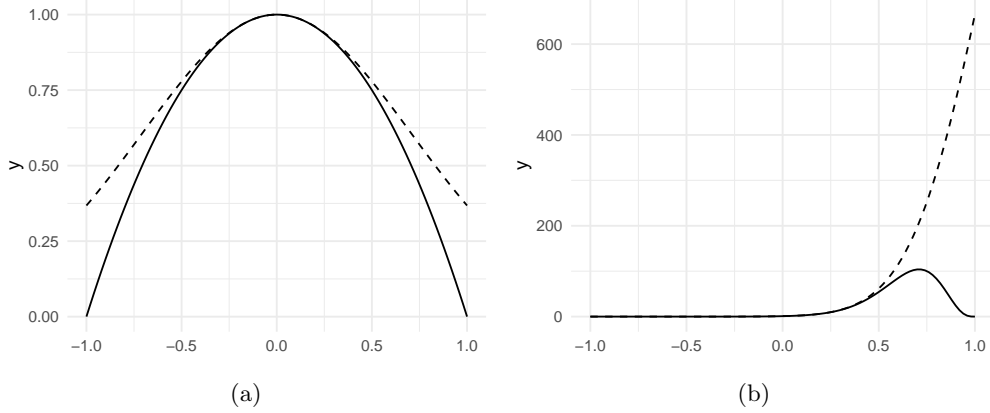


Figure 1: Simple proposal based on one region with $\kappa = 10$ and $d = 10$: (a) displays weight functions w (solid) and \bar{w} (dashed); (b) displays unnormalized densities f_0 (solid) and h_0 (dashed).

An alternative VWS proposal will handle $d \in \{2, 3\}$ and obtain practical rejection rates for a wide range of κ and d . We will make use of the linear VWS approach described in Section 3.3 with numerical optimization to identify c^* in (12) in (14). Let $\alpha_0 = -1 + \epsilon$ and $\alpha_N = 1 - \epsilon$ for a small $\epsilon > 0$ so that $\Omega = (-1, 1)$ is to be partitioned into regions of the form $(\alpha_{j-1}, \alpha_j]$, where $\alpha_0 < \dots < \alpha_N$. Rewrite the target distribution as

$$f(x) = \frac{(\kappa/2)^{d/2-1} (1-x^2)^{(d-3)/2} \exp(\kappa x)}{\sqrt{\pi} \cdot I_{d/2-1}(\kappa) \cdot \Gamma((d-1)/2)} \cdot \mathbf{I}(-1 < x < 1) \\ \propto (1-x^2)^{(d-3)/2} \exp(\kappa x) \cdot \mathbf{I}(-1 < x < 1),$$

which suggests a decomposition into weight function $w(x) = (1-x^2)^{(d-3)/2}$ and base density $g(x) = (e^\kappa - e^{-\kappa})^{-1} \kappa e^{\kappa x} \cdot \mathbf{I}(-1 < x < 1)$. Density g corresponds to the distribution $\text{Exp}_{(-1,1)}$ from Example 2. The trivial minorizer discussed in Remark 1 may be computed as $\xi_j = \psi\{G(\alpha_j) - G(\alpha_{j-1})\}$, where G is the CDF in (15). For the majorizer, we note that

$$\log w(x) = \frac{1}{2}(d-3) \log(1-x^2), \\ \frac{d}{dx} \log w(x) = -(d-3) \frac{x}{1-x^2}, \\ \frac{d^2}{dx^2} \log w(x) = -(d-3) \frac{1+x^2}{(1-x^2)^2}.$$

Therefore, w is log-convex if $d < 3$, log-concave if $d > 3$, and a constant if $d = 3$. Note that $\frac{d^2}{dx^2} \log f_0(x) = -(d-3)(1+x^2)/(1-x^2)^2$ so that the target f is also log-convex, log-concave, or constant under the same conditions. Using log-convexity or log-concavity, the majorizer for w on \mathcal{D}_j may be taken as $\bar{w}_j = \exp\{\bar{\beta}_{0j} + \bar{\beta}_{1j}x\}$ with constants $\bar{\beta}_{0j}$ and $\bar{\beta}_{1j}$ selected according to Section 3.3. From Example 2, density g_j corresponds to distribution $\text{Exp}_{(-\alpha_{j-1}, \alpha_j)}(\kappa + \bar{\beta}_{j1})$ so that draws $T \sim g_j$ may be generated via the inverse CDF method. Note that $w(x) = \infty$ for $x \in \{-1, 1\}$ when $d < 3$, so we take the approach discussed in Remark 3 of truncating the support to $(-1 + \epsilon, 1 - \epsilon)$. The value of ϵ is taken to be 10^{-4} except in Section 4.2 where it is 10^{-6} .

Figure 2 displays several cases of the target density f with $\kappa \in \{0.1, 10\}$ and $d \in \{2, 3, 4\}$. Figure 3 displays 50,000 draws of a three-dimensional VMF distribution with $\kappa \in \{0.1, 10\}$ constructed from variates from rejection sampling on f . To generate such draws from f , let us consider the UW rejection sampler and three variations of the VWS sampler: VS, constant VWS, and linear VWS discussed in Section 3. VS and constant VWS each requires very little derivation while linear VWS requires more work but is expected to

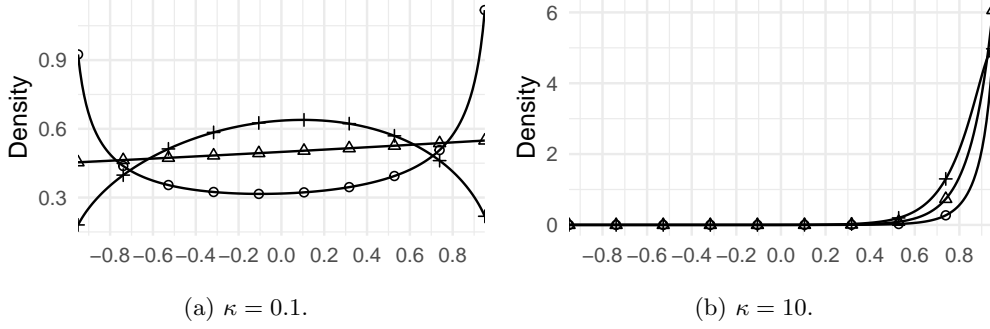


Figure 2: Density (19) used to draw from the VMF distribution: $d = 2$ (\circ), $d = 3$ (\triangle), and $d = 4$ ($+$).

be more efficient. Figure 4 displays each of the three mixture proposals for $N = 5$ regions with $d = 2$ and $\kappa = 0.75$ along with the unnormalized target density. The interior knots $\alpha_1, \dots, \alpha_4$ in each case have been selected according to the rule of thumb described in Section 3.4. Overall rejection rates $1 - \psi/\psi_N$ of the VS, constant VWS, and linear VWS samplers are 93.93%, 93.59%, and 76.42%, respectively. The contribution ρ_ℓ from (17) is displayed within each region in Figure 4; the trivial minorizer has been used to compute $\underline{\xi}_\ell$ for all three proposals. After refining to only $N = 5$ regions, it is apparent that linear VWS achieves a notably better rejection rate than the other two variations.

A small study has been carried out to compare overall rejection rates for the UW, VS, constant VWS, and linear VWS methods. We consider $d \in \{2, 4, 5\}$ and $\kappa \in \{0.1, 10\}$. Note that we have skipped $d = 3$ because it is an easier case with the quadratic term vanishing from f . In each setting, the UW rejection rate is computed empirically using 50,000 draws. The VS, constant VWS, and linear VWS samplers are based on N regions, where N is adapted from a single region to 100 regions using the method from Section 3.4. The process of adapting from one to 100 regions is repeated 100 times to express randomness used in the selection. Figure 5 displays the median rejection rate on the log-scale as $\log(1 - \psi/\psi_N)$, taken over the 100 repetitions, along with confidence band for the 2.5% and 97.5% quantiles. The UW sampler is seen to be quite efficient when $\kappa = 0.1$ but rejects more frequently when $\kappa = 10$. In the case that $\kappa = 10$ and $d = 5$, the rejection rate is 23.9%. The VS and constant VWS samplers perform comparably, with constant VWS slightly more efficient for $\kappa = 10$. For all nine settings of d and κ , VS and constant VWS achieve a rejection rate of $\exp(-2.47) = 8.5\%$ or lower with 100 regions; this is competitive with the efficiency of UW when $\kappa \geq 1$. VWS linear outperforms VS and constant VWS in all settings and achieves rejection rates several orders of magnitude smaller. To improve upon the rejection rate of UW, linear VWS requires nearly $N = 100$ when $\kappa = 0.1$ but only a small N when $\kappa = 10$. In this application, the effort to derive and implement linear VWS yields a rejection sampler which can achieve a very low rejection rate with consistent performance over the family of target distributions.

4.2 Approximate Computation of Probabilities

Proposition 2 established that proposal h may be useful in approximating probabilities under f when bound (4) can be made small. To illustrate, let us consider the probability that $\mathbf{V}_0 \sim \text{VMF}_d(\boldsymbol{\mu}_0, \kappa)$ lies in the nonnegative orthant $A = \{\mathbf{v} \in \mathbb{R}^d : \mathbf{v} \geq 0\}$. Using transformation (18),

$$\begin{aligned}
 \mathbb{P}(\mathbf{V}_0 \in A) &= \mathbb{P}\left(X \geq 0, U_1 \sqrt{1 - X^2} \geq 0, \dots, U_{d-1} \sqrt{1 - X^2} \geq 0\right) \\
 &= \mathbb{P}(X \geq 0, U_1 \geq 0, \dots, U_{d-1} \geq 0) \\
 &= \mathbb{P}(U_1 \geq 0, \dots, U_{d-1} \geq 0) \mathbb{P}(X \geq 0) \\
 &= 2^{-(d-1)} \mathbb{P}(X \geq 0).
 \end{aligned}$$

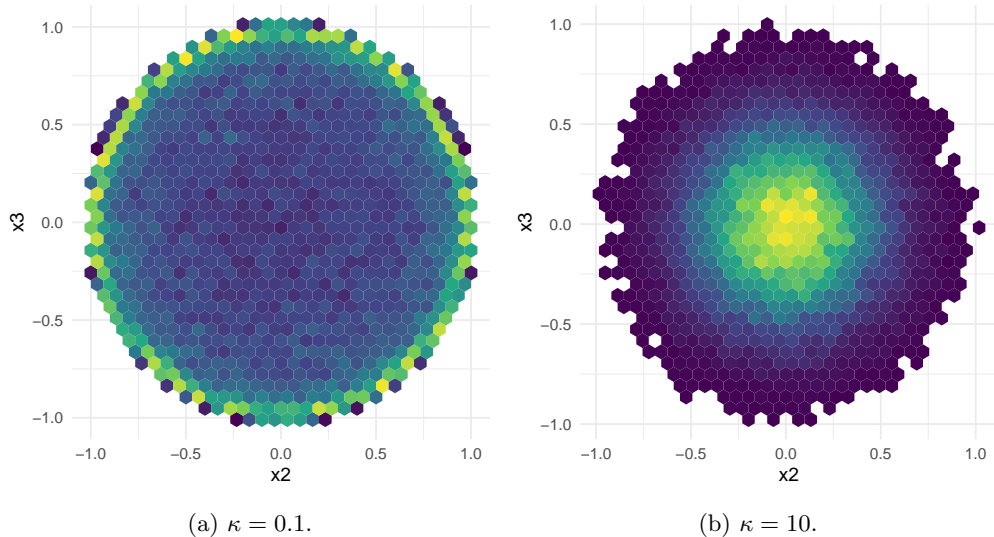


Figure 3: Empirical distribution of 50,000 draws of $\mathbf{V}_0 \sim \text{VMF}_3(\boldsymbol{\mu}_0, \kappa)$, projected to the x_2 - x_3 plane from $\boldsymbol{\mu}_0 = (1, 0, 0)$. Yellow bins contain a larger number of points while purple bins contain fewer points.

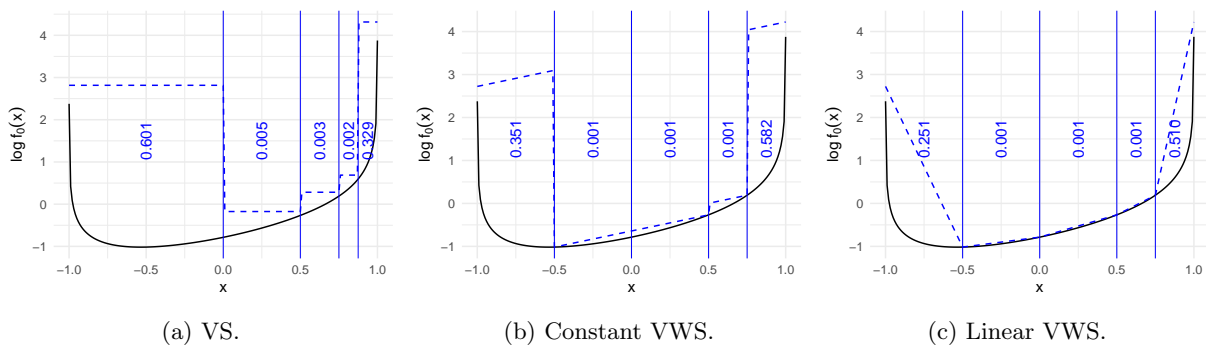


Figure 4: Unnormalized proposal log-density $\log h_0(x)$ for three VWS proposals (dashed blue curves) with $d = 2$, $\kappa = 0.75$ and $N = 5$ regions, and target log-density $\log f_0(x)$ (solid black curve). Solid horizontal blue lines are locations of interior knots $\alpha_1, \dots, \alpha_4$. The value displayed within a region is its contribution ρ_ℓ to the rejection rate.

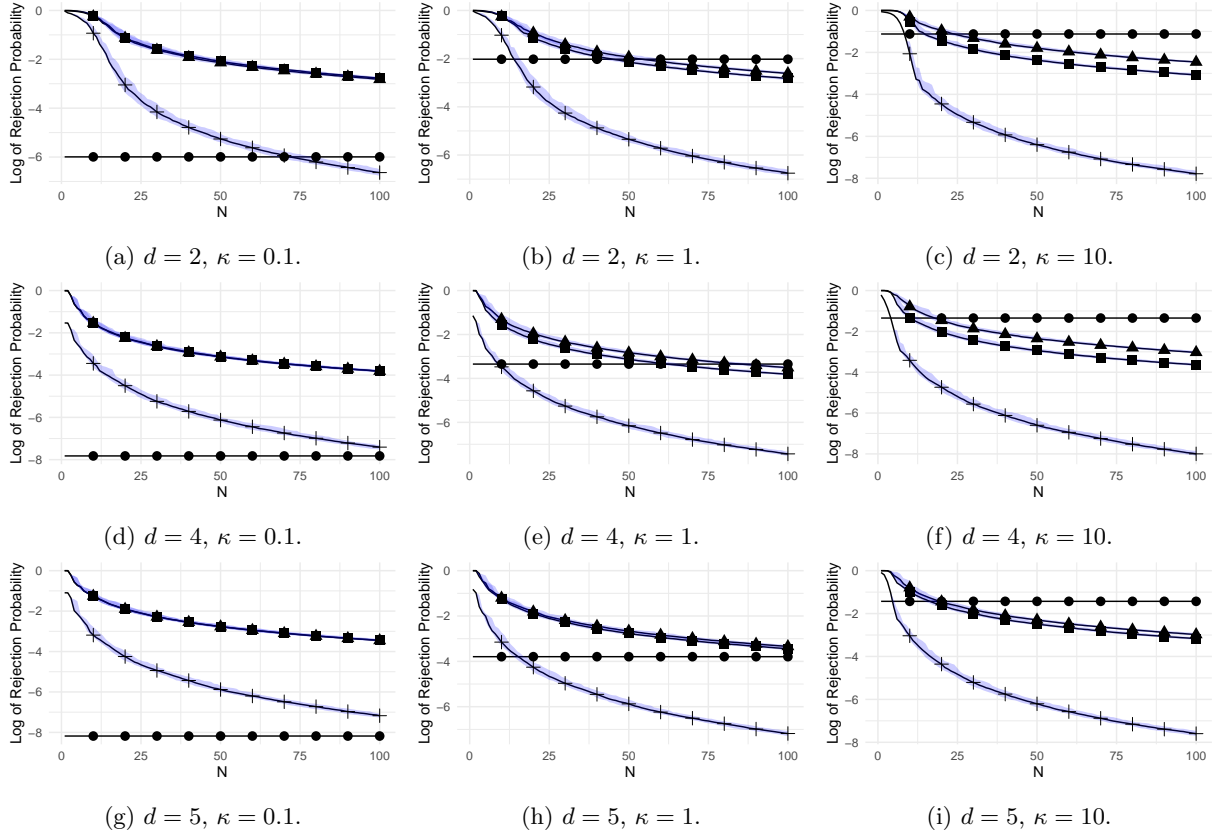


Figure 5: Log of rejection probability, $\log(1 - \psi/\psi_N)$, for $d = 2, 4, 5$ and $\kappa = 0.1, 1, 10$ using UW (\bullet), VS (\blacktriangle), constant VWS (\blacksquare), and linear VWS ($+$) samplers.

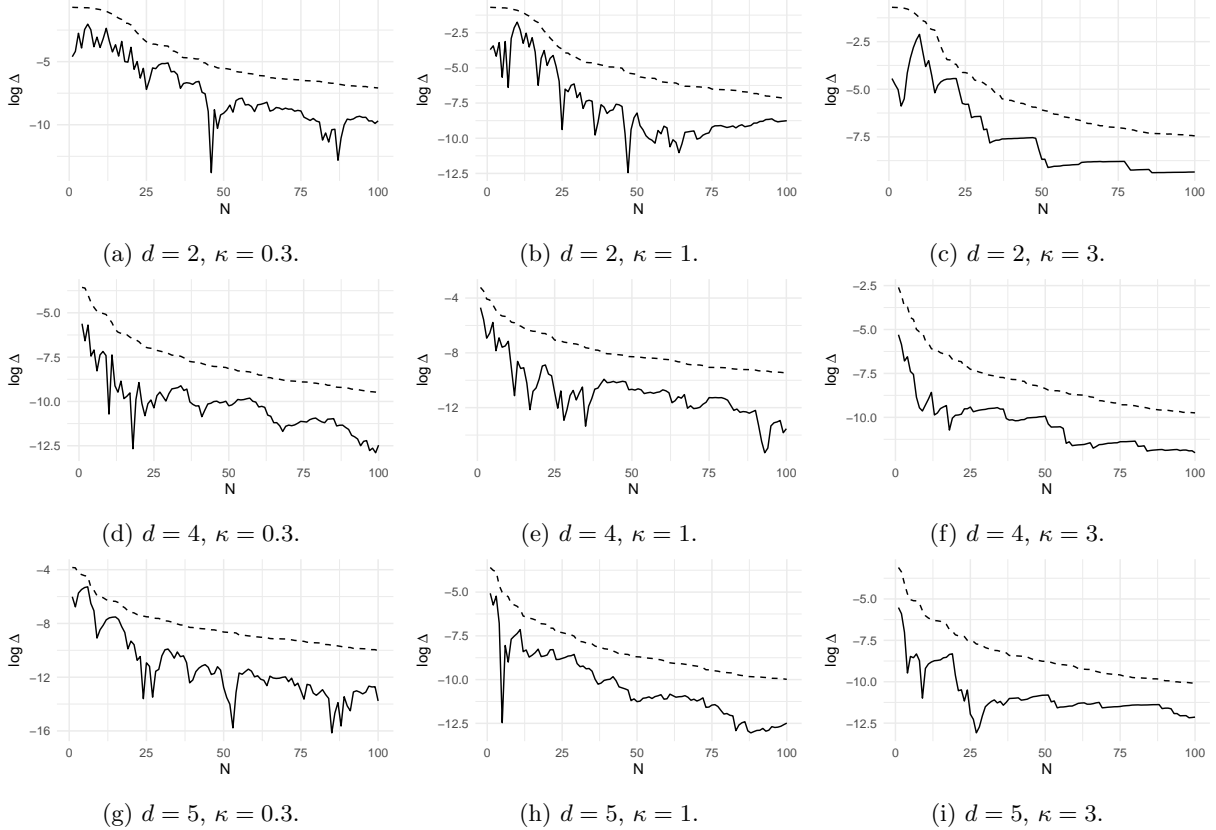


Figure 6: Log of approximation error Δ using linear VWS proposal (solid curve) versus upper bound (dashed curve) given in (21).

Similarly, let $\tilde{\mathbf{V}}_0 = (\tilde{X}, [1 - \tilde{X}^2]^{1/2} \cdot \mathbf{U})$ with $\tilde{X} \sim h$ so that $\mathbb{P}(\tilde{\mathbf{V}}_0 \in A) = 2^{-(d-1)} \mathbb{P}(\tilde{X} \geq 0)$. The bound (4) gives

$$\begin{aligned}
 \Delta &:= |\mathbb{P}(\tilde{\mathbf{V}}_0 \in A) - \mathbb{P}(\mathbf{V}_0 \in A)| \\
 &= 2^{-(d-1)} |\mathbb{P}(\tilde{X} \geq 0) - \mathbb{P}(X \geq 0)| \\
 &\leq 2^{-(d-1)} (1 - \psi/\psi_N).
 \end{aligned} \tag{21}$$

Let us again consider the linear VWS proposal from Section 4.1. Figure 6 displays the realized approximation error Δ and its upper bound (21), on the log-scale, for $\kappa \in \{0.3, 1, 3\}$ and $d \in \{2, 4, 5\}$ as N increases from 1 to 100. The realized approximation error is often significantly smaller than the bound. Proposal h is adapted using the method in Section 3.4 for each increment of N . Increases in Δ from increasing N are possible due to refinements in h which occur outside of event A . Such refinements make the error within A relatively larger and might be avoided if $\mathbb{P}(\mathbf{V}_0 \in A)$ is the only aspect of h which is of interest. With $N = 100$ regions, the largest error of the nine settings of κ and d is $\Delta = \exp(-8.754) \approx 1.58 \times 10^{-4}$ with $d = 2$ and $\kappa = 1$; for comparison, the value of the probability here is $\mathbb{P}(\mathbf{V}_0 \in A) \approx 0.3902$.

4.3 A Bayesian Application

A third setting which can make use of vertical weighted strips is in a Bayesian analysis with independent and identically distributed VMF outcomes. [Damien and Walker \(1999\)](#) propose a full Bayesian treatment

for circular data ($d = 2$) based on Gibbs sampling with data augmentation. Nuñez-Antonio and Gutiérrez-Peña (2005) propose a Bayesian treatment for $d \geq 2$ based on sampling-importance-resampling. Taghia et al. (2014) explore variational approximation to the posterior for VMF as well as finite mixtures of VMF densities. We will develop a rejection sampler based on vertical weighted strips for the VMF setting; although the posterior does not follow a familiar distribution, samples can be generated from it exactly without resorting to MCMC.

Suppose $\mathbf{v}_1, \dots, \mathbf{v}_n$ are an independent and identically distributed sample from $\text{VMF}_d(\boldsymbol{\mu}, \kappa)$ with unknown $\kappa > 0$ and $\boldsymbol{\mu} \in \mathbb{S}^d$. A conjugate prior in this setting is given by

$$\pi(\boldsymbol{\mu}, \kappa) \propto \left[\frac{\kappa^{d/2-1}}{I_{d/2-1}(\kappa)} \right]^{c_0} \exp(\kappa R_0 \mathbf{m}_0^\top \boldsymbol{\mu})$$

where $c_0 \geq 0$, $R_0 \geq 0$, and $\mathbf{m}_0 \in \mathbb{S}^d$ (Mardia and El-Atoum, 1976). Upon observing $\mathbf{v}_1, \dots, \mathbf{v}_n$, the posterior distribution for $[\boldsymbol{\mu}, \kappa \mid \mathbf{v}_1, \dots, \mathbf{v}_n]$ is

$$\begin{aligned} \pi^{(n)}(\boldsymbol{\mu}, \kappa) &\propto \pi(\boldsymbol{\mu}, \kappa) \left[\frac{\kappa^{d/2-1}}{I_{d/2-1}(\kappa)} \right]^n \exp \left\{ \kappa \boldsymbol{\mu}^\top \sum_{i=1}^n \mathbf{v}_i \right\} \\ &= \left[\frac{\kappa^{d/2-1}}{I_{d/2-1}(\kappa)} \right]^{c_0+n} \exp \{ \kappa R_n \boldsymbol{\mu}^\top \mathbf{m}_n \} \end{aligned}$$

where $\mathbf{m}_n = R_n^{-1}(\sum_{i=1}^n \mathbf{v}_i + R_0 \mathbf{m}_0)$ and R_n is the Euclidean norm of $\sum_{i=1}^n \mathbf{v}_i + R_0 \mathbf{m}_0$. Therefore, $\pi(\boldsymbol{\mu}, \kappa)$ is seen to be a conjugate prior. Notice that

$$\pi^{(n)}(\boldsymbol{\mu}, \kappa) \propto \left[\frac{\kappa^{d/2-1}}{I_{d/2-1}(\kappa)} \right]^{c_0+n-1} \frac{I_{d/2-1}(\kappa R_n)}{I_{d/2-1}(\kappa)} f_{\text{VMF}}(\boldsymbol{\mu} \mid \mathbf{m}_n, \kappa R_n)$$

is the product of conditional distribution $[\boldsymbol{\mu} \mid \kappa, \mathbf{v}_1, \dots, \mathbf{v}_n] \sim \text{VMF}(\boldsymbol{\mu} \mid \mathbf{m}_n, \kappa R_n)$ and marginal $[\kappa \mid \mathbf{v}_1, \dots, \mathbf{v}_n]$ with unnormalized density $f_0(\kappa) = \left[\kappa^{d/2-1} / I_{d/2-1}(\kappa) \right]^{c_0+n-1} I_{d/2-1}(\kappa R_n) / I_{d/2-1}(\kappa)$. Therefore, exact generation of variates from the posterior may be accomplished by first drawing κ from f_0 then $\boldsymbol{\mu}$ from $\text{VMF}(\boldsymbol{\mu} \mid \mathbf{m}_n, \kappa R_n)$. The latter has been explored in Section 4.1, so we now focus on the target f_0 . Consider the decomposition $f_0(\kappa) = w(\kappa)g(\kappa)$ with $g(\kappa) = \tau e^{-\tau\kappa} \cdot \mathbb{I}(\kappa > 0)$ is the density of the Exponential distribution with a $\tau > 0$ of our choosing and

$$\begin{aligned} w(\kappa) &= \tau^{-1} \cdot e^{\tau\kappa} \left[\frac{\kappa^{d/2-1}}{I_{d/2-1}(\kappa)} \right]^{c_0+n-1} \frac{I_{d/2-1}(\kappa R_n)}{I_{d/2-1}(\kappa)} \\ &= \tau^{-1} \cdot e^{-\kappa(1-R_n-\tau)} \left[\frac{\kappa^{d/2-1}}{e^\kappa \mathcal{I}_{d/2-1}(\kappa)} \right]^{c_0+n-1} \frac{\mathcal{I}_{d/2-1}(\kappa R_n)}{\mathcal{I}_{d/2-1}(\kappa)}, \end{aligned}$$

where $\mathcal{I}_\nu(x) = e^{-x} I_\nu(x)$ is the exponentially scaled Bessel function. The exponential scaled Bessel $\mathcal{I}_\nu(x)$ can be computed with `besselI` in R and is useful for working on the log-scale to avoid precision issues due to large magnitude numbers. To carry out VWS sampling from f_0 , we opt for the constant majorizer described in Section 3.2, using numerical optimization to find the minimum and maximum of $\log w(\kappa)$ on each region \mathcal{D}_j , and take $\tau = 0.01$ so that the proposal is not closely concentrated around zero. We will make use of bound (4) and avoid computing the normalizing constant ψ of f_0 .

Let us consider a dataset from Appendix B2 of Fisher et al. (1993) with $n = 26$ measurements of magnetic remanence in specimens of Palaeozoic red-beds from Argentina. Measurements are initially given as declination / inclination coordinates $(\theta_{i1}, \theta_{i2})$ in degrees and transformed to \mathbb{R}^3 using

$$v_{i1} = \sin(\vartheta_{i2}) \cos(\vartheta_{i1}), \quad v_{i2} = \sin(\vartheta_{i2}) \sin(\vartheta_{i1}), \quad v_{i3} = \cos(\vartheta_{i2}),$$

where $\vartheta_{i1} = (360^\circ - \theta_{i1})\pi/180^\circ$ and $\vartheta_{i2} = (90^\circ + \theta_{i2})\pi/180^\circ$. A benefit of a rejection sampling approach—such as VWS—is that accepted draws will be an exact sample from the target. We take hyperparameters $c_0 = 0$ and $R_0 = 0$ to match Example 5.4 of Nuñez-Antonio and Gutiérrez-Peña (2005).

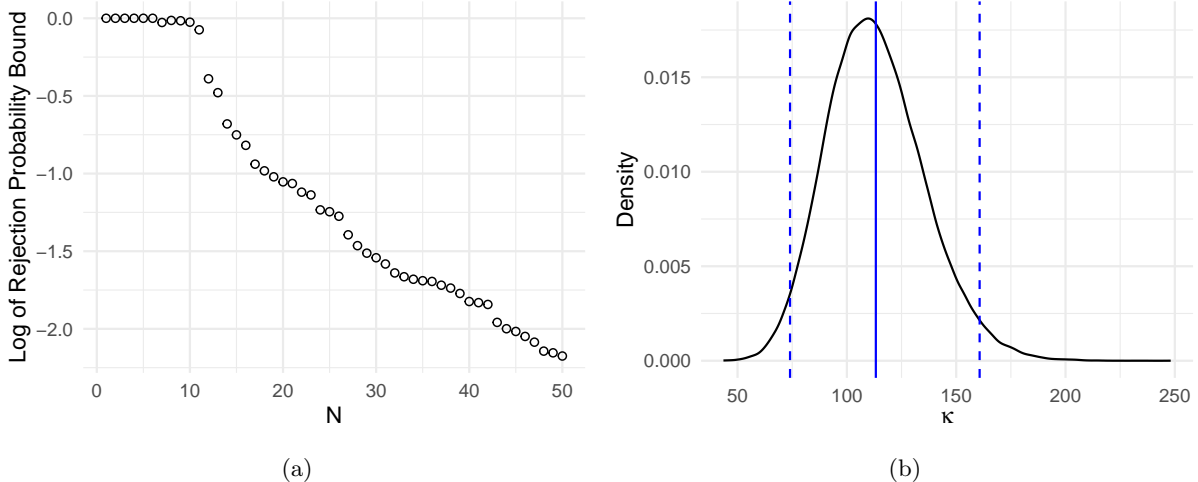


Figure 7: Results for posterior $[\kappa \mid \mathbf{v}_1, \dots, \mathbf{v}_n]$. (a) Bound (4) for rejection probability on the log-scale as N increases from 1 to 50. (b) empirical density of accepted draws (solid curve) with mean (solid vertical line) and 2.5% and 97.5% quantiles (dashed vertical lines).

Figure 7 displays the results of rejection sampling. The bound (4) shown in Figure 7a reduces to 11.4% with $N = 50$ regions. Using this proposal, 6,363 rejections were encountered to obtain a sample of 100,000 (5.98% rejection). The empirical density of the posterior based on the accepted draws is displayed in Figure 7b. An estimate of κ based on the posterior mean is $\hat{\kappa} = 113.24$ and an associated 95% credible interval based on 2.5% and 97.5% quantiles is (74.00, 160.72). For comparison, consider the MLE computed by numerical maximization of the log-likelihood; here, we transform from three Euclidean pre-parameters $\zeta = (\zeta_1, \zeta_2, \zeta_3)$ to $(\kappa, \boldsymbol{\mu})$ to enforce $\kappa > 0$ and $\boldsymbol{\mu} \in \mathbb{S}^d$ with unconstrained optimization. We obtain the estimate $\hat{\kappa} = 113.24$ and an associated 95% confidence interval (77.07, 166.24).

5 Illustrations with Gaussian Process

Gaussian Processes (GPs) are widely used in statistics and machine learning to model unspecified functions. There is extensive literature on applications including curve fitting (Shi and Choi, 2011), computer simulation experiments (Gramacy, 2020), and kriging in spatial statistics (Christianson et al., 2023). We will consider two examples involving Bayesian analysis of GPs which can be expressed as univariate targets that are amenable to a VWS approach. Section 5.1 uses VWS to fit a curve based on observations from the curve with error. Section 5.2 considers VWS in a spatial regression model with an additional linear term. Although these may be considered toy examples—as only one covariance parameter is taken to be unknown—they may be interesting as cases where the posterior has an unfamiliar form but can be sampled exactly without MCMC and with relatively few rejections.

5.1 Learning a Function from Noisy Observations

Let $\zeta : \mathbb{R}^d \rightarrow \mathbb{R}$ be a function of interest to be modeled by a GP and $k : \mathbb{R}^d \times \mathbb{R}^d \rightarrow [0, \infty)$ be a covariance kernel. Denote (\mathbf{x}_i, y_i) , $i = 1, \dots, n$, as training data where $\mathbf{x}_i \in \mathbb{R}^d$ is an input and $y_i \in \mathbb{R}$ is a corresponding noisy observation. Similarly, let $(\mathbf{x}_{0i}, y_{0i})$, $i = 1, \dots, n_0$, be test data where y_{0i} may or may not be observed. Consider the model

$$y_i = \zeta(\mathbf{x}_i) + \epsilon_i, \quad \epsilon_i \sim N(0, \sigma^2), \quad \zeta \sim \text{GP}(0, k(\cdot, \cdot)), \quad \sigma^2 \sim \text{Uniform}(a_\sigma, b_\sigma), \quad (22)$$

with hyperparameters $0 < a_\sigma < b_\sigma < \infty$. Define the design matrices

$$\mathbf{X} = (\mathbf{x}_1 \cdots \mathbf{x}_n)^\top \quad \text{and} \quad \mathbf{X}_0 = (\mathbf{x}_{01} \cdots \mathbf{x}_{0n_0})^\top,$$

the vectors

$$\mathbf{y} = (y_1, \dots, y_n), \quad \zeta(\mathbf{X}) = [\zeta(\mathbf{x}_1), \dots, \zeta(\mathbf{x}_n)]^\top, \quad \text{and} \quad \zeta(\mathbf{X}_0) = [\zeta(\mathbf{x}_{01}), \dots, \zeta(\mathbf{x}_{0n_0})]^\top,$$

and the covariance matrices

$$\mathbf{K}_{11} = (k(\mathbf{x}_i, \mathbf{x}_j)) \in \mathbb{R}^{n \times n}, \quad \mathbf{K}_{01} = (k(\mathbf{x}_{0i}, \mathbf{x}_j)) \in \mathbb{R}^{n_0 \times n}, \quad \mathbf{K}_{00} = (k(\mathbf{x}_{0i}, \mathbf{x}_{0j})) \in \mathbb{R}^{n_0 \times n_0}, \quad (23)$$

and $\mathbf{K}_{10} = \mathbf{K}_{01}^\top$. Model (22) may be written in matrix form as

$$\mathbf{y} = \zeta(\mathbf{X}) + \boldsymbol{\epsilon}, \quad \boldsymbol{\epsilon} \sim \mathbf{N}(\mathbf{0}, \sigma^2 \mathbf{I}), \quad \zeta(\mathbf{X}) \sim \mathbf{N}(\mathbf{0}, \mathbf{K}_{11}), \quad \sigma^2 \sim \text{Uniform}(a_\sigma, b_\sigma).$$

With the spectral decomposition $\mathbf{U}\boldsymbol{\Lambda}\mathbf{U}^\top$ of \mathbf{K}_{11} , where $\boldsymbol{\Lambda} = \text{Diag}(\lambda_1, \dots, \lambda_n)$, we have $\sigma^2 \mathbf{I} + \mathbf{K}_{11} = \mathbf{U}[\sigma^2 \mathbf{I} + \boldsymbol{\Lambda}]\mathbf{U}^\top$. Consider transforming from \mathbf{y} to $\mathbf{z} = \mathbf{U}^\top \mathbf{y}$ so that $[\mathbf{z} \mid \sigma^2] \sim \mathbf{N}(\mathbf{0}, \sigma^2 \mathbf{I} + \boldsymbol{\Lambda})$ has independent elements. The log-posterior of the transformed observations is seen to be

$$\pi(\sigma^2 \mid \mathbf{z}) \propto (2\pi)^{-n/2} \left[\prod_{i=1}^n (\sigma^2 + \lambda_i)^{-1/2} \right] \exp \left\{ -\frac{1}{2} \sum_{i=1}^n \frac{z_i^2}{\sigma^2 + \lambda_i} \right\} \cdot \mathbf{I}(\sigma^2 \in [a_\sigma, b_\sigma]). \quad (24)$$

To sample from (24) using VWS, consider a decomposition with weight function

$$\log w(\sigma^2) = -\frac{n}{2} \log(2\pi) - \frac{1}{2} \sum_{i=1}^n \log(\sigma^2 + \lambda_i) - \frac{1}{2} \sum_{i=1}^n \frac{z_i^2}{\sigma^2 + \lambda_i} \quad (25)$$

from the likelihood, and base distribution g the density of prior $\text{Uniform}(a_\sigma, b_\sigma)$. Notice that any computationally intensive matrix operations have been avoided in (25) so that they will not need to be repeated in the sampler, though such an operation may be needed to initially obtain \mathbf{U} and $\boldsymbol{\Lambda}$. The first and second derivatives of $\log w(\sigma^2)$ are

$$\begin{aligned} \frac{d}{d\sigma^2} \log w(\sigma^2) &= \frac{1}{2} \sum_{i=1}^n \frac{z_i^2 - \sigma^2 - \lambda_i}{(\sigma^2 + \lambda_i)^2}, \quad \text{and} \\ \frac{d^2}{d(\sigma^2)^2} \log w(\sigma^2) &= \sum_{i=1}^n \frac{\sigma^2/2 + \lambda_i/2 - z_i^2}{(\sigma^2 + \lambda_i)^3}. \end{aligned} \quad (26)$$

so that w is log-convex when (26) is positive and log-concave when (26) is negative. The linear VWS majorizer and minorizer in Section 3.3 may be used, provided that we are careful to partition the support into regions which are entirely log-convex or entirely log-concave. The j th reweighted & truncated base density is obtained in Example 3 as

$$g_j(\sigma^2) = \frac{\beta_{j1} \cdot e^{\bar{\beta}_{j1} \sigma^2}}{e^{\bar{\beta}_{j1} \alpha_j} - e^{\bar{\beta}_{j1} \alpha_{j-1}}} \mathbf{I}(\alpha_{j-1} < \sigma^2 \leq \alpha_j),$$

which is the density of the $\text{Exp}_{(\alpha_{j-1}, \alpha_j)}(\bar{\beta}_{j1})$ distribution. Knot selection and rejection sampling from VWS may now be carried out to yield draws $\sigma^{2(r)}$, $r = 1, \dots, R$ from posterior (25). Draws from the posterior predictive distribution $[\zeta(\mathbf{X}_0) \mid \mathbf{z}]$ may then be obtained by drawing $\zeta^{(r)}(\mathbf{X}_0)$ from

$$\mathbf{N}(\mathbf{K}_{01} \mathbf{U}(\sigma^2 \mathbf{I} + \boldsymbol{\Lambda})^{-1} \mathbf{z}, \mathbf{K}_{00} - \mathbf{K}_{01} \mathbf{U}(\sigma^2 \mathbf{I} + \boldsymbol{\Lambda})^{-1} \mathbf{U}^\top \mathbf{K}_{10}) \quad (27)$$

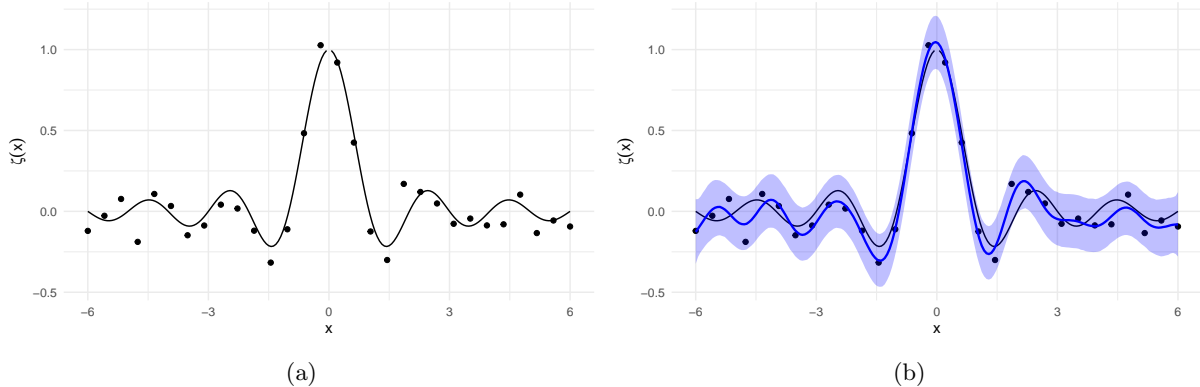


Figure 8: Observed data and predictions from GP: (a) displays true ζ and observed y_1, \dots, y_n ; (b) overlays posterior mean (blue curve) and associated 95% pointwise interval (blue band).

for each sampled variate $\sigma^{2(r)}$ of σ^2 . Note that (27) is obtained from the distribution

$$[\mathbf{y}, \zeta(\mathbf{X}_0) \mid \sigma^2] \sim \mathcal{N} \left(\begin{bmatrix} \mathbf{0} \\ \mathbf{0} \end{bmatrix}, \begin{bmatrix} \sigma^2 \mathbf{I} + \mathbf{K}_{11} & \mathbf{K}_{10} \\ \mathbf{K}_{01} & \mathbf{K}_{00} \end{bmatrix} \right)$$

and applying the transformation $\mathbf{z} = \mathbf{U}^\top \mathbf{y}$.

Let us consider a simulated example based on the sinc function $\zeta(x) = \sin(\pi x)/(\pi x)$, where we observe $n = 25$ outcomes $y_i = \zeta(x_i) + \epsilon_i$ with $\epsilon_i \stackrel{\text{iid}}{\sim} \mathcal{N}(0, 0.1^2)$ and x_i on an evenly spaced grid on the interval $[-6, 6]$. We select hyperparameters to be $a_\sigma = 0$ and $b_\sigma = 10^6$ and take k to be the squared exponential covariance kernel $k(\mathbf{x}, \mathbf{x}') = \exp\{-\frac{1}{2}\|\mathbf{x} - \mathbf{x}'\|^2\}$. Figure 8a displays the observed data and the true $\zeta(x)$. Figure 9a plots the second derivative (26) of $\log w(\sigma^2)$; here, a single root is seen at $\tilde{\sigma}^2 = 0.0153$ so that w is log-concave for $\sigma^2 < \tilde{\sigma}^2$ and log-convex otherwise. Furthermore, (26) is seen to decrease to zero as σ^2 continues to increase. Therefore, taking $\mathcal{D}_1 = [a_\sigma, \tilde{\sigma}^2)$ and $\mathcal{D}_2 = [\tilde{\sigma}^2, b_\sigma)$ as the initial two regions ensures that w is entirely either log-concave or log-convex in any further partitions. Figure 9b displays bound (4) for VWS sampler as N is increased from 1 to 100 using the knot selection described in Section 3.4. With $N = 100$ regions, we achieve a bound of $\exp(-6.777) \approx 0.114\%$. During sampling, 27 proposals were rejected to obtain a sample of 50,000 draws: an observed rejection rate of 0.054%. Figure 9c plots the empirical density of draws generated from the sampler. For comparison, we fit the model in Stan using the No-U-Turn sampler (Carpenter et al., 2017). The empirical density of draws from Stan was nearly indistinguishable from that of the VWS sampler and is therefore not shown. Coding the model in Stan using log-posterior (24) leads to very fast sampling. The main advantage of VWS over Stan in this problem is the guarantee that draws are an exact sample from the posterior. Finally, Figure 8b displays the posterior predictive mean of $\zeta(x)$ for x on a fine grid on $[-6, 6]$, along with associated pointwise 95% intervals using 0.025 and 0.975 quantiles from the posterior predictive distribution.

A similar approach to VWS sampling can be taken using other covariance kernels where parameters within the kernel are fixed. It can also be used with other priors on σ^2 which coalesce with the linear majorization, such as an exponential family as in Example 1.

5.2 Spatial Regression Model

The spatial linear regression model presented in Chapter 6 of Banerjee et al. (2015) is an extension of the GP discussed in Section 5.1. We will consider a variation of the model whose posterior can be sampled with univariate VWS. Suppose $\mathbf{x}_i \in \mathbb{R}^d$ are locations on a spatial domain with fixed covariate $\mathbf{s}(\mathbf{x}_i) \in \mathbb{R}^m$ and

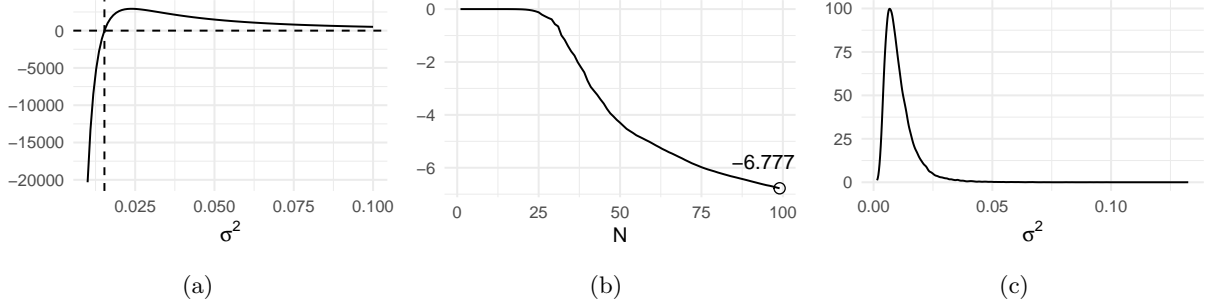


Figure 9: (a) Second derivative of $\log w(\sigma^2)$ for simulated GP dataset, with root $\bar{\sigma}^2 = 0.0153$ (vertical dashed line). (b) Upper bound for rejection rate on the log-scale. (c) Empirical density of saved draws.

observation y_i , $i = 1, \dots, n$, and

$$\begin{aligned} y_i &= \mathbf{s}(\mathbf{x}_i)^\top \boldsymbol{\beta} + \zeta(\mathbf{x}_i) + \epsilon_i, \quad \epsilon_i \stackrel{\text{iid}}{\sim} N(0, \sigma^2), \quad \zeta \sim \text{GP}(0, k(\cdot, \cdot)), \\ \boldsymbol{\beta} &\sim N(\mathbf{0}, \mathbf{Q}_\beta^-), \quad \sigma^2 \sim \text{IG}(a_\sigma, b_\sigma), \end{aligned} \quad (28)$$

where \mathbf{Q}_β is a precision matrix and \mathbf{Q}_β^- is its generalized inverse. Using similar matrix notation as in Section 5.1, model (28) becomes

$$\begin{aligned} \mathbf{y} &= \mathbf{S}\boldsymbol{\beta} + \boldsymbol{\zeta} + \boldsymbol{\epsilon}, \quad \boldsymbol{\epsilon} \sim N(\mathbf{0}, \sigma^2 \mathbf{I}), \quad \boldsymbol{\zeta} \sim N(\mathbf{0}, \mathbf{K}), \\ \boldsymbol{\beta} &\sim N(\mathbf{0}, \mathbf{Q}_\beta^-), \quad \sigma^2 \sim \text{IG}(a_\sigma, b_\sigma), \end{aligned} \quad (29)$$

where $\mathbf{S} = [s(\mathbf{x}_1), \dots, s(\mathbf{x}_n)]^\top$, $\boldsymbol{\zeta} = [\zeta(\mathbf{x}_1), \dots, \zeta(\mathbf{x}_n)]^\top$, and $\mathbf{K} = (k(\mathbf{x}_i, \mathbf{x}_j)) \in \mathbb{R}^{n \times n}$.

Banerjee et al. (2015, Section 6.3) considers a forest inventory dataset from the Bartlett Experimental Forest (BEF). Here, the spatial domain is a $d = 2$ dimensional region within the forest, the outcome y_i is taken to be log-transformed total tree biomass, and there are five covariates in $\mathbf{s}(\mathbf{x}_i)$: slope, elevation, tasseled cap brightness, greenness, and wetness measured from satellite imagery. After fitting model (28) to the point-level data, predictions of biomass may be computed on a fine grid over the domain. Following Banerjee et al. (2015, Section 6.3), let $\mathbf{Q}_\beta = \mathbf{0}$ so that $\boldsymbol{\beta}$ has a flat prior on \mathbb{R}^m and let k be an exponential kernel $k(\mathbf{x}, \mathbf{x}') = \gamma^2 \exp\{-\phi \|\mathbf{x} - \mathbf{x}'\|\}$. Parameters γ^2 and σ^2 are referred to as the partial sill and nugget in the spatial setting, respectively.

The R package `spBayes` (Finley et al., 2015) provides several functions to support inference for this class of model. The function `bayesGeostatExact` samples exactly from the posterior of $[\boldsymbol{\beta}, \sigma^2, \gamma^2 \mid \mathbf{y}]$, assuming that ϕ and the ratio σ^2/γ^2 are fixed at given values. The function `spLM` allows all three covariance parameters— σ^2 , γ^2 , and ϕ —to be unknown and included in inference using a Metropolis-Hastings approach. Variables $\boldsymbol{\beta}$ and $\boldsymbol{\zeta}$ are marginalized out of the target posterior to reduce dimension of the parameter space during sampling but their draws may be recovered afterward.

Let us consider a variation of this setting where ϕ and γ^2 are fixed, σ^2 is unknown, and the ratio σ^2/γ^2 is unspecified. We take $\phi = 0.014$, as in Banerjee et al. (2015, Section 6.3), and $\gamma = 1$. Integrating over $\boldsymbol{\beta}$ and $\boldsymbol{\zeta}$ gives the likelihood

$$\begin{aligned} \pi(\mathbf{y} \mid \sigma^2) &= \int_{\mathbb{R}^m} \int_{\mathbb{R}^n} f_N(\mathbf{y} \mid \mathbf{S}\boldsymbol{\beta} + \boldsymbol{\zeta}, \sigma^2 \mathbf{I}) f_N(\boldsymbol{\zeta} \mid \mathbf{0}, \mathbf{K}) d\boldsymbol{\zeta} d\boldsymbol{\beta} \\ &= (2\pi)^{-(n-m)/2} |\mathbf{Q}|^{-1/2} |\mathbf{S}^\top \mathbf{Q} \mathbf{S}|^{-1/2} \exp\left\{-\frac{1}{2} \mathbf{y}^\top \mathbf{Q} \mathbf{y}\right\} \exp\left\{-\frac{1}{2} \mathbf{y}^\top \mathbf{Q} \mathbf{S} [\mathbf{S}^\top \mathbf{Q} \mathbf{S}]^{-1} \mathbf{S}^\top \mathbf{Q} \mathbf{y}\right\}, \end{aligned} \quad (30)$$

where $\mathbf{Q} = (\sigma^2 \mathbf{I} + \mathbf{K})^{-1}$. To sample from the posterior

$$\pi(\sigma^2 \mid \mathbf{y}) \propto \pi(\mathbf{y} \mid \sigma^2) \cdot f_{\text{IG}}(\sigma^2 \mid a_\sigma, b_\sigma),$$

using a VWS approach, let base $g(\sigma^2)$ be the density of $\text{IG}(a_\sigma, b_\sigma)$ and weight function $w(\sigma^2)$ be (30). Consider the constant VWS majorizer from Section 3.2. The normalizing constant ψ of $\pi(\sigma^2 | \mathbf{y})$ appears to be intractable so we also use the minorizer from Section 3.2 to compute bound (4). The maximum and minimum of w for each region of the partition are computed numerically using the `optim` function in R via the Nelder-Mead method. To decrease computational burden within numerical optimization, let $\mathbf{U}(\sigma^2 \mathbf{I} + \mathbf{\Lambda})^{-1} \mathbf{U}^\top$ be the spectral decomposition of \mathbf{Q} as in Section 5.1 so that (30) may be expressed on the log-scale as

$$\begin{aligned} \log w(\sigma^2) = & -\frac{n-m}{2} \log(2\pi) + \frac{1}{2} \sum_{i=1}^n \log(\sigma^2 + \lambda_i) - \frac{1}{2} \log |\mathbf{W}^\top (\sigma^2 \mathbf{I} + \mathbf{\Lambda})^{-1} \mathbf{W}| - \frac{1}{2} \sum_{i=1}^n \frac{z_i^2}{\sigma^2 + \lambda_i} \\ & - \frac{1}{2} \mathbf{z}^\top (\sigma^2 \mathbf{I} + \mathbf{\Lambda})^{-1} \mathbf{W} [\mathbf{W}^\top (\sigma^2 \mathbf{I} + \mathbf{\Lambda})^{-1} \mathbf{W}]^{-1} \mathbf{W}^\top (\sigma^2 \mathbf{I} + \mathbf{\Lambda})^{-1} \mathbf{z}, \end{aligned}$$

where $\mathbf{W} = \mathbf{U}^\top \mathbf{S}$ and $\mathbf{z} = \mathbf{U}^\top \mathbf{y}$ are free of the unknown parameter σ^2 . After obtaining draws from the posterior $[\sigma^2 | \mathbf{y}]$, draws of $\boldsymbol{\beta}$ can be recovered from

$$\begin{aligned} \pi(\boldsymbol{\beta} | \sigma^2, \mathbf{y}) & \propto \pi(\mathbf{y} | \boldsymbol{\beta}, \sigma^2) \pi(\boldsymbol{\beta}) \\ & \propto \exp \left\{ -\frac{1}{2} (\mathbf{y} - \mathbf{S}\boldsymbol{\beta})^\top (\sigma^2 \mathbf{I} + \mathbf{K})^{-1} (\mathbf{y} - \mathbf{S}\boldsymbol{\beta}) \right\}, \end{aligned}$$

which is a multivariate normal distribution with mean $\boldsymbol{\Gamma}_\beta^{-1} \mathbf{S}^\top (\sigma^2 \mathbf{I} + \mathbf{K})^{-1} \mathbf{y}$ and precision $\boldsymbol{\Gamma}_\beta = \mathbf{S}^\top (\sigma^2 \mathbf{I} + \mathbf{K})^{-1} \mathbf{S}$. Draws of $\boldsymbol{\zeta}$ can subsequently be recovered from

$$\begin{aligned} \pi(\boldsymbol{\zeta} | \boldsymbol{\beta}, \sigma^2, \mathbf{y}) & \propto \pi(\mathbf{y} | \boldsymbol{\beta}, \boldsymbol{\zeta}, \sigma^2) \pi(\boldsymbol{\zeta}) \\ & \propto \exp \left\{ -\frac{1}{2\sigma^2} (\mathbf{y} - \mathbf{S}\boldsymbol{\beta} - \boldsymbol{\zeta})^\top (\mathbf{y} - \mathbf{S}\boldsymbol{\beta} - \boldsymbol{\zeta}) \right\} \exp \left\{ -\frac{1}{2\sigma^2} \boldsymbol{\zeta}^\top \mathbf{K}^{-1} \boldsymbol{\zeta} \right\}, \end{aligned}$$

which is a multivariate normal distribution with mean $\sigma^{-2} \boldsymbol{\Gamma}_\zeta^{-1} (\mathbf{y} - \mathbf{S}\boldsymbol{\beta})$ and precision $\boldsymbol{\Gamma}_\zeta = \sigma^{-2} \mathbf{I} + \mathbf{K}^{-1}$. Finally, suppose $\mathbf{X}_0 = (\mathbf{x}_{01} \cdots \mathbf{x}_{0n_0})^\top$ are locations for a test set with corresponding design matrix $\mathbf{S}_0 = [\mathbf{s}(\mathbf{x}_{01}) \cdots \mathbf{s}(\mathbf{x}_{0n_0})]^\top$, function values $\boldsymbol{\zeta}_0 = [\zeta(\mathbf{x}_{01}) \cdots \zeta(\mathbf{x}_{0n_0})]^\top$, and covariance kernel matrices \mathbf{K}_{ab} for $r, s \in \{0, 1\}$ defined as in (23). Draws from $[\boldsymbol{\zeta}_0 | \mathbf{y}]$ may be obtained from previous draws using

$$\pi(\boldsymbol{\zeta}_0 | \boldsymbol{\zeta}, \boldsymbol{\beta}, \sigma^2, \mathbf{y}) \propto \pi(\boldsymbol{\zeta}_0 | \boldsymbol{\zeta}),$$

which is a multivariate normal distribution with mean $\mathbf{K}_{01} \mathbf{K}_{11}^{-1} \boldsymbol{\zeta}$ and variance $\mathbf{K}_{00} - \mathbf{K}_{01} \mathbf{K}_{11}^{-1} \mathbf{K}_{10}$. Draws of $\boldsymbol{\zeta}_0$ may be combined with corresponding draws of $\mathbf{S}_0 \boldsymbol{\beta}$ to obtain a sample from the overall posterior predictive distribution.

Figure 10 presents several results from the VWS sampler. Figure 10a displays bound (4) as N is increased from 1 to 100 using the knot selection method from Section 3.4. With $N = 100$ regions, the bound is $\exp(-3.154) \approx 4.27\%$. To generate 50,000 draws from the sampler, 1,103 proposals (2.16%) were rejected. The empirical distribution of the saved draws is displayed in Figure 10b.

6 Conclusions

This paper has explored vertical weighted strips, a generalization of the vertical strips method to construct proposals for rejection sampling. Regarding the target as a weighted density provides additional flexibility in constructing the proposal. Several examples demonstrated that practical samplers can be achieved; very efficient samplers were obtained in some cases with the support partitioned into a moderate number of regions.

We focused on two particular majorizers: one based on a constant and one based on a linear function on the logarithmic scale. A source of inspiration for more useful inequalities may be in the minorization-maximization (MM) literature (e.g. Lange, 2016), where minorization is used to construct a sequence of surrogates to a complicated likelihood function which are more readily maximized to obtain an MLE.

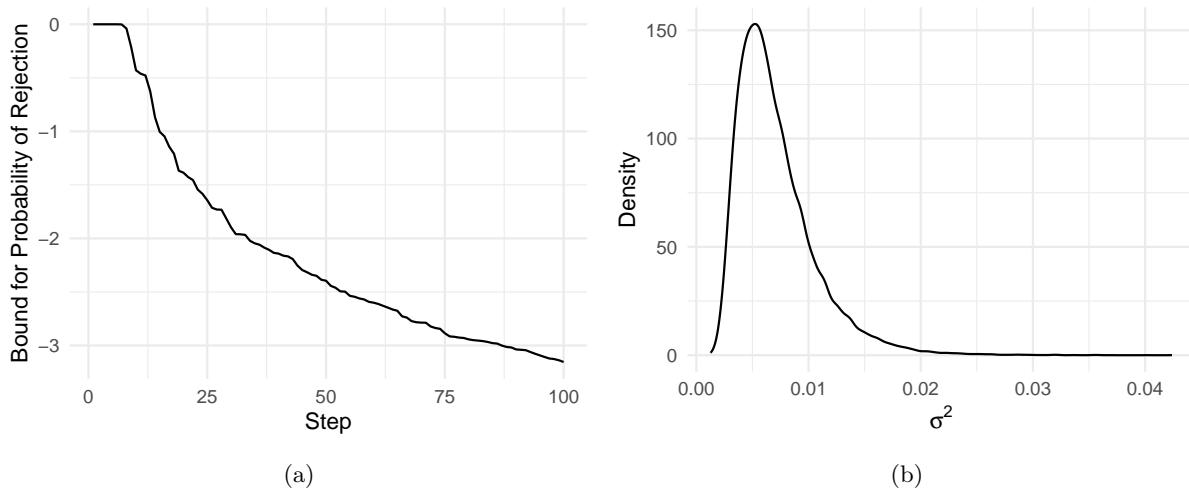


Figure 10: VWS sampler for BEF data analysis. (a) Bound (4) for rejection probability as N increases. (b) empirical density of draws.

The univariate setting of this paper most readily applies to multivariate sampling within the context of a Gibbs sampler. Here, vertical weighted strips may be used to generate exact draws from unfamiliar univariate conditionals. There is a tradeoff between proposal construction time and sampling time: often only one draw is needed in each iteration of the Gibbs sampler so that a slightly higher rejection rate may be preferable to spending more time to construct the proposal each iteration. For reference, one round of knot selection for the illustrations in Sections 4 and 5 takes on the order of seconds (or less) on a workstation with an AMD Ryzen 5600G with six cores and 16MB of cache.

There is also potential for virtual weighted strips methodology to be applied directly to multivariate settings. Rather than intervals which have been used in the univariate case, it may be necessary to partition into along multiple dimensions—e.g., with hyperrectangles—in such settings. Generation of proposed draws from subsequent reweighted and truncated base distributions must then be practical for a usable sampler. This approach appears viable for some problems which are of interest to the authors and is an area for future work.

Acknowledgments

We thank Daniel Weinberg (U.S. Census Bureau) for providing a review of the manuscript.

References

- J H. Ahrens. Sampling from general distributions by suboptimal division of domains. *Grazer Mathematische Berichte*, 319:20, 1993. ISSN 1016-7692.
- J.H. Ahrens. A one-table method for sampling from continuous and discrete distributions. *Computing*, 54(20):127–146, 1995.
- S. Banerjee, B. P. Carlin, and A. E. Gelfand. *Hierarchical modeling and analysis for spatial data*. CRC Press, 2nd edition, 2015.
- Bob Carpenter, Andrew Gelman, Matthew D. Hoffman, Daniel Lee, Ben Goodrich, Michael Betancourt, Marcus Brubaker, Jiqiang Guo, Peter Li, and Allen Riddell. Stan: A probabilistic programming language. *Journal of Statistical Software*, 76(1):1–32, 2017.

- Ryan B. Christianson, Ryan M. Pollyea, and Robert B. Gramacy. Traditional kriging versus modern Gaussian processes for large-scale mining data. *Statistical Analysis and Data Mining: The ASA Data Science Journal*, 16(5):488–506, 2023.
- Paul Damien and Stephen Walker. A full Bayesian analysis of circular data using the von Mises distribution. *The Canadian Journal of Statistics*, 27(2):291–298, 1999.
- Luc Devroye. *Non-Uniform Random Variate Generation*. Springer, 1986.
- M. Evans and T. Swartz. Random variable generation using concavity properties of transformed densities. *Journal of Computational and Graphical Statistics*, 7(4):514–528, 1998.
- Andrew O. Finley, Sudipto Banerjee, and Alan E. Gelfand. spBayes for large univariate and multivariate point-referenced spatio-temporal data models. *Journal of Statistical Software*, 63(13):1–28, 2015.
- N.I. Fisher, T. Lewis, and B.J.J. Embleton. *Statistical Analysis of Spherical Data*. Cambridge University Press, 1993.
- W. R. Gilks and P. Wild. Adaptive rejection sampling for Gibbs sampling. *Journal of the Royal Statistical Society: Series C (Applied Statistics)*, 41(2):337–348, 1992.
- W. R. Gilks, N. G. Best, and K. K. C. Tan. Adaptive rejection Metropolis sampling within Gibbs sampling. *Journal of the Royal Statistical Society: Series C (Applied Statistics)*, 44(4):455–472, 1995.
- Dilan Görür and Yee Whye Teh. Concave-convex adaptive rejection sampling. *Journal of Computational and Graphical Statistics*, 20(3):670–691, 2011.
- Robert B. Gramacy. *Surrogates: Gaussian Process Modeling, Design and Optimization for the Applied Sciences*. Chapman Hall/CRC, Boca Raton, Florida, 2020.
- W. Hörmann. A note on the performance of the “Ahrens algorithm”. *Computing*, 69(1):83–89, 2002.
- Kurt Hornik and Bettina Grün. movMF: An R package for fitting mixtures of von Mises-Fisher distributions. *Journal of Statistical Software*, 58(10):1–31, 2014.
- Gerhard Kurz and Uwe D. Hanebeck. Stochastic sampling of the hyperspherical von Mises–Fisher distribution without rejection methods. In *2015 Sensor Data Fusion: Trends, Solutions, Applications (SDF)*, pages 1–6, 2015.
- Kenneth Lange. *MM Optimization Algorithms*. Society for Industrial and Applied Mathematics, Philadelphia, PA, 2016.
- K. V. Mardia and S. A. M. El-Atoum. Bayesian inference for the von Mises-Fisher distribution. *Biometrika*, 63(1):203–206, 1976.
- Kanti V. Mardia and Peter E. Jupp. *Directional Statistics*. Wiley, 1999.
- George Marsaglia and Wai Wan Tsang. The ziggurat method for generating random variables. *Journal of Statistical Software*, 5(8):1–7, 2000.
- Luca Martino, Jesse Read, and David Luengo. Independent doubly adaptive rejection Metropolis sampling within Gibbs sampling. *IEEE Transactions on Signal Processing*, 63(12):3123–3138, 2015.
- Luca Martino, Roberto Casarin, Fabrizio Leisen, and David Luengo. Adaptive independent sticky MCMC algorithms. *EURASIP Journal on Advances in Signal Processing*, 2018(1), 2018a.
- Luca Martino, David Luengo, and Joaquín Míguez. *Independent Random Sampling Methods*. Springer, 2018b.

- Mervin E. Muller. A note on a method for generating points uniformly on N -dimensional spheres. *Communications of the ACM*, 2(4):19–20, 1959.
- G. Nuñez-Antonio and E. Gutiérrez-Peña. A Bayesian analysis of directional data using the von Mises-Fisher distribution. *Communications in Statistics - Simulation and Computation*, 34(4):989–999, 2005.
- W.K. Pang, Z.H. Yang, S.H. Hou, and P.K. Leung. Non-uniform random variate generation by the vertical strip method. *European Journal of Operational Research*, 142(3):595–609, 2002.
- G. P. Patil and C. R. Rao. Weighted distributions and size-biased sampling with applications to wildlife populations and human families. *Biometrics*, 34(2):179–189, 1978.
- Arthur Pewsey and Eduardo García-Portugués. Recent advances in directional statistics. *TEST*, 30(1):1–58, 2021.
- R Core Team. *R: A Language and Environment for Statistical Computing*. R Foundation for Statistical Computing, Vienna, Austria, 2023. URL <https://www.R-project.org>.
- Andrew M. Raim. Direct sampling with a step function. *Statistics and Computing*, 33(22), 2023.
- Christian P. Robert and George Casella. *Monte Carlo Statistical Methods*. Springer, 2nd edition, 2004.
- Jian Qing Shi and Taeryon Choi. *Gaussian process regression analysis for functional data*. CRC Press, 2011.
- Jalil Taghia, Zhanyu Ma, and Arne Leijon. Bayesian estimation of the von-Mises Fisher mixture model with variational inference. *IEEE Transactions on Pattern Analysis and Machine Intelligence*, 36(9):1701–1715, 2014.
- Michail Tsagris and Manos Papadakis. Forward regression in R: From the extreme slow to the extreme fast. *Journal of Data Science*, 16(4):771–780, 2018.
- Gary Ulrich. Computer generation of distributions on the M -sphere. *Journal of the Royal Statistical Society: Series C (Applied Statistics)*, 33(2):158–163, 1984.
- John von Neumann. Various techniques in connection with random digits. In A.S. Householder, G.E. Forsythe, and H.H. Germond, editors, *Monte Carlo Methods*, National Bureau of Standards Applied Mathematics Series, pages 36–38. U.S. Government Printing Office, Washington, DC, 1951.
- Stephen G. Walker, Purushottam W. Laud, Daniel Zantedeschi, and Paul Damien. Direct sampling. *Journal of Computational and Graphical Statistics*, 20(3):692–713, 2011.
- Andrew T. A. Wood. Simulation of the von Mises Fisher distribution. *Communications in Statistics—Simulation and Computation*, 23(1):157–164, 1994.